BASELINE CHARACTERIZATION OF ENVIRONMENTAL CONDITIONS LEADING UP TO MARINE PROTECTED AREA ESTABLISHMENT IN THE NORTH-CENTRAL COAST STUDY REGION

William J. Sydeman[1,2], Sarah Ann Thompson[1,3], Marisol Garcia-Reyes[1], and Mati Kahru[2]

[1]Farallon Institute for Advanced Ecosystem Research
Petaluma, CA 94952
www.faralloninstitute.org
www.faralloninstitute2@wordpress.com

[2]Integrative Oceanography, Scripps Institution of Oceanography
La Jolla, CA 95060

[3]Climate Impacts Group, University of Washington, Seattle, WA 98115

Revised Final Report: 1 October 2013

This page intentionally left blank.

Table of Contents

Tables and Figures

A. Assessment of Project Goals and Accomplishments

Recognizing past and ongoing change in environmental conditions (climatological, oceanographic, and ecological), the Monitoring Enterprise requested an assessment of environmental conditions leading up to MPA implementation in the NCC region. This work was designed to promote a better understanding of baseline monitoring results. As many if not most biological populations in the region respond to environmental variation, evaluating coupled climate-ecosystem variability is essential to detect and subsequently attribute changes in MPAs to management actions. In this project, we addressed this specific need for the NCC MPA biological monitoring program.

Fundamentally, our project was a task of integration. To accomplish this project, we proposed to develop and report upon a suite of integrated *multivariate indicators* of (a) "ocean climate", and (b) biological populations and productivity, which together may serve to characterize the state of the regional ecosystem.

Using our *Integrated Marine Ecological Database* (**IMED**; Farallon Inst., unpubl.), we focused on developing *multivariate ocean climate indicators* (hereafter *MOCI*). *MOCI* were based on a compilation of 16 well-known large-scale to regional indicators (details provided in our final report). As proposed, we compiled data for each season from 1990-2010, and produced seasonal *MOCI* using Principal Component/Empirical Orthogonal Function analysis. As proposed, we were able to test the relationships between *MOCI* and lower and upper trophic level ecosystem components including a measurement of phytoplankton biomass (chl-a concentration – a combined product from OCTS, SeaWiFS, and MODIS) and seabird productivity (breeding success of 4 species from the Farallon Islands).

As proposed, we analyzed each of the indicator data sets for trends in "state" (mean) and "variability" (variance). In comparison with other environmental syntheses, this analysis is significant in that (a) it focuses on the NNC region (previous work has been on the scale of the entire California Current), (b) it includes indicators that have yet to be integrated in other ecosystem status reports (e.g., surface currents from the State of California's HF radar array), and (c) the *MOCI* are intuitive and interpretable and as such should be accessible to the MPA management community (Monitoring Enterprise, CDFW).

We also proposed to augment **IMED** with new data collected during the baseline monitoring efforts, but unfortunately were not able to integrate these data because the data are not yet available from other project PIs. We could have foreseen this issue with the timing of availability of new NCC MPA monitoring data, but during the proposal process, this did not occur to us, the ME, or other project PIs.

Overall, we accomplished most project goals and are satisfied with project results (statistical integration of environmental indicators). This information should be of considerable value to the State of California for understanding and evaluating results of baseline MPA monitoring in the NCC region. We have also submitted a paper based on this project for publication in the journal *Progress in Oceanography*.

B. Executive Summary – Integrated Ecosystem Assessment (Sydeman and Thompson, Revised 1 October 2013)

1. California's nearshore marine life is responsive to year-to-year and longer-term changes in ocean conditions. In particular, growth/size, production, and abundance of fish and other taxa are known to change with variation in water temperature, upwelling-favorable winds, and currents. Therefore, baseline information on variability in ocean conditions is required to understand and evaluate changes in populations in this region. This context is critical to monitoring population change and adaptive management of Marine Protected Areas (MPA) in California. Without a simultaneous assessment of the effects of ocean conditions, it will be difficult to formally attribute changes in populations to the protection afforded by MPA designations.

2. In this report, we develop and explore comprehensive indicators of temporal variability in ocean conditions over a 21-year period preceding the establishment of MPAs along California's north-central coast (NCC). To test the relevance of these indicators to populations, we relate them to a few key biological data sets that are representative of marine life within and outside NCC MPA.

3. To develop ocean-climate indicators, we selected, compiled and analyzed 16 well-known atmospheric and oceanographic measurements that represent key large-scale drivers and regional attributes of the coastal physical environment. These include drivers of ocean-climate variability from the tropical Pacific (e.g., El Niño - Southern Oscillation) and north Pacific (e.g., Pacific Decadal Oscillation), as well as regional atmospheric and ocean conditions such as wind stress, sea surface temperature, salinity, and a novel time series of surface currents from the State of California's new HF radar array. While the indicators are based on large- to regional-scale measurements, they have consequences for marine life at the local (MPA) scale and thus are important to biological monitoring, management evaluations, and adaptive management.

4. In this project, we designed and implemented seasonal indicators using a multivariate statistical technique used to synthesize groups of related variables known as Principal Component Analysis (PCA). PCA allows one to understand relationships between similar variables taken from different locations, as well as combine variables in a comprehensive and synthetic manner. We refer to this compilation of variables as seasonal "Multivariate Ocean Climate Indicators" (MOCI).

5. Our analysis of ocean conditions over the 21-year period leading up to MPA establishment in the NCC study region indicates weakening of the ENSO cycle resulting in fewer and less intense El Niño events, and a strengthening of sub-arctic influences on the region including a major cooling represented by the Pacific Decadal Oscillation (PDO). Corresponding to these changes, the Northern Oscillation Index (NOI) strengthened, leading to enhanced upwelling-

favorable wind stress as well as air and ocean surface temperature cooling. These conditions are conducive to population growth for species with temperate or sub-arctic zoogeographic affinities, such as many fish species now protected by MPAs. This indicates that population recovery may be enhanced by the prevailing ocean conditions leading up to MPA implementation.

6. Corresponding to the recent increases in upwelling-favorable winds and decreases in ocean temperature, phytoplankton biomass also increased in the NCC study region. The positive trend observed in phytoplankton biomass could be important for other marine life under study in NCC MPA as it indicates greater biomass at the base of the food chain. MOCI also related well to seabird productivity. We recommend additional tests of the applicability of MOCI to populations, including populations studied during monitoring activities of central coast MPA.

7. Our study supports a conclusion of enhanced sub-arctic influences and upwelling intensification in north-central California over the past two decades, and that these changes are contributing to greater lower trophic level biomass. Our analyses provide context necessary to evaluate responses in local coastal ecosystems to recent changes in fishing and other practices within MPA. Linking changes in the MOCI to newly obtained biological observations from MPA monitoring is warranted to separate the effects of ocean-climate variability from changes in fishing and other anthropogenic pressures on these coastal ecosystems and populations.

8. Regular updating of MOCI will be necessary to advance analyses of coupled climate-ecosystem change and management evaluations in the NCC and other study regions of California. It would also be of great value to consider the skill of MOCI in predicting biological variables from NCC MPA monitoring once these data are made accessible to the research and management communities.

9. Adaptive management of NCC MPA may be enhanced by the greater understanding of ocean conditions revealed by MOCI and other indicators of environmental variability. MOCI provide the environmental “backdrop” for the evaluation of population change, thereby providing context with which to interpret monitoring results within and outside MPA. If population changes within MPA match those of control or reference sites, this could indicate that environmental factors (as described by MOCI) are driving population changes. If population changes do not match, this could indicate that management (protection) is having a stronger impact. In this manner, managers may be able to ascribe the statistical variation in populations to either environmental (ocean) conditions or management actions.

C. Final Revised Report

BASELINE CHARACTERIZATION OF ENVIRONMENTAL CONDITIONS LEADING UP TO MARINE PROTECTED AREA ESTABLISHMENT IN THE NORTH-CENTRAL COAST STUDY REGION

William J. Sydeman[1,2], Sarah Ann Thompson[1,3], Marisol Garcia-Reyes[1], and Mati Kahru[2]

[1]Farallon Institute for Advanced Ecosystem Research
Petaluma, CA 94952
www.faralloninstitute.org
www.faralloninstitute2@wordpress.com

[2]Integrative Oceanography, Scripps Institution of Oceanography
La Jolla, CA 95060

[3]Climate Impacts Group, University of Washington, Seattle, WA 98115

1 October 2013

1. Introduction

Ocean-climate variability has been shown to strongly affect marine life, including plankton, fish, and top predators, with clear applications in fisheries, wildlife and ecosystem management (Hjort, 1914; Cury et al., 2008; Carr et al., 2011). Compared to many of the world's seas, the effects of ocean-climate variability on the California Current ecosystem (CCE) have been particularly well-studied (Peña and Bograd, 2007). This marine realm, situated off the west coast of Canada, the U.S., and Baja California, Mexico, is affected by basin-scale atmospheric-oceanic coupling due to the combined effects of El Niño Southern Oscillation events (ENSO; Lenarz et al., 1995; McPhaden et al., 2006) and the decadal-scale North Pacific Gyre Oscillation (Di Lorenzo et al., 2008) and Pacific Decadal Oscillation (PDO; Mantua et al., 1997). Regional coastal and offshore upwelling, operating from daily to decadal time scales, also affect biotic variability of the CCE (Huyer, 1983; García-Reyes and Largier, 2010, 2012). Mechanistically, currents associated with tropical and extra-tropical transport bring waters of varying characteristics into the system (Chelton et al., 1982). Subsequently, regional upwelling and its vertical and offshore displacement operate on these water masses, dispersing nutrients and plankton, which in turn determines primary and secondary productivity (Checkley and Barth, 2009). Thus, to understand how climate variability relates to marine life in the CCE, consideration of the interactive effects of horizontal (currents) and vertical (upwelling) transport is required. Although a variety of indicators are available to proxy these processes, rarely have they been combined in a holistic manner to examine bio-physical interactions (but see Hemery et al., 2008).

The need for a comprehensive approach to ocean-climate indicators increased recently when the State of California established a network of 124 Marine Protected Areas (MPAs) and 15 special closures in which fisheries and other human activities were either curtailed or eliminated entirely. This management began with the implementation of 29 MPAs along the central California coast in 2007 followed by 25 MPAs along the central-northern coast in 2010. In 2012, 50 south coast and 20 north coast MPAs were implemented. In total, ~852 mi^2 and ~16% of California's coastal waters are now protected in no-take marine reserves and limited-take marine conservation areas (www.dfg.ca.gov/mlpa). California's MPAs are located in coastal to neritic habitats typically within three miles from shore, near offshore islands (such as the Farallon Islands), and above major subsurface topographies (e.g., Monterey Canyon). Since MPAs restrict fisheries and other human uses of marine species and habitats, MPA implementation was controversial. Therefore, in conjunction with implementation, an evaluation program designed to provide information on biotic responses to reductions in fisheries mortality and other factors was initiated. Fieldwork for these management-oriented evaluations began in 2008 along the central coast and in 2011 along the north-central coast.

Monitoring the outcome of reduced fishing when MPAs are established may be complicated by environmental variability which can confound interpretations of biotic change. For example, many of the focal *Sebastes* spp. respond to variation in large-scale and local ocean climate with effects on growth (Black et al., 2010) and proxies of reproductive success (Ralston et al., 2013). To place these recently obtained biological observations in an environmental context, we designed and implemented a framework for ocean-climate indicators for the central and north-central California Current by combining a suite of well-known indicators using multivariate statistical procedures (see also Mackas et al., 2007; Hemery et al., 2008). Our principal goal was to provide an assessment of environmental conditions leading up to MPA establishment in the mid-late 2000s. Because CCE biota respond to seasonal variation in environmental conditions (e.g., Hooff and Peterson, 2006; Black et al., 2010, 2011; Thompson et al., 2012), we produced indicators for intra-annual variability. The utility of complex multivariate indicators can be challenged if they are difficult to interpret or do not accurately represent known environmental variability (Rice and Rochet, 2005). Therefore, based on the literature, we developed a series of *a priori* expectations to evaluate multivariate indicators. These include El Niño conditions that affected the region in 1992-1993, 1997-1998, 2003, and 2009-2010 (Bjorkstedt et al., 2010), the warm-water non-El Niño event of 2005 (GRL Special Section, 2006), and strong La Niña conditions in 1999 and 2008. These conditions have been well described in previous publications, but to date there have been no attempts to create multivariate ocean-climate indicators or evaluate how well these indicators represent such variability. If indicators match known variability, arguably they would be interpretable and representative, key attributes for useful and valid ecological indicators (Levin et al., 2009). To test the utility of our multivariate ocean-climate indicators (hereafter MOCI, see Hemery et al. 2008), we related them to two initial lower and upper trophic-level biological indicators. We will provide a more comprehensive analysis of biological responses to MOCI in a future report. Here, we focus on indicator development and a description of environmental conditions over the 21-year period 1990-2010.

2. Methods

We focused data synthesis on 1990 through 2010 as this period followed the putative regime shifts of 1989-1990 (Hare and Mantua, 2000) and 1976-1997 (McGowan et al., 2003). Others have suggested another regime shift in 1998-1999 (Bond et al., 2003; Peterson and Schwing, 2003), but the persistence of this shift remains equivocal. We selected a total of 16 basin- (SOI, MEI, ONI, NPI, PDO, NPGO, NOI, and California Current flow (two individual measurements)) and regional-scale (Upwelling Index, wind stress, sea level, SST, salinity, surface air temperature, and precipitation) atmospheric and oceanographic indicators for synthesis (Table 1, see below for descriptions). We evaluated environmental conditions by exploring variability on different time scales. When MPAs are established, fisheries mortality is reduced immediately. Therefore, relatively short-term biotic responses are possible assuming rapidly responding response parameters are monitored. In considering the potential for rapid biological responses, we focused on understanding the status of the environment on seasonal, interannual, and bi/triennial scales. However, while some rapid biological responses are possible, long-lived species may not show short-term changes. This is certainly true for the *Sebastes* spp. of interest in this ecosystem – changes in the populations of these species are likely only on decadal scales. Therefore, in this context, we focused on understanding trends in the environment and decadal-scale variability. Last, we examine the potential for our multivariate ocean climate indicators to predict biological responses by investigating relationships with two well-known biological indicators:

seabird reproductive success (Ainley et al., 1995; Sydeman et al., 2001, 2006, 2009) and chlorophyll-a concentrations (Kahru et al., 2012).

2.1 Data

2.1.1 Indicators of Transport from the Tropics

Indicators of the warm El Niño phase of the ENSO cycle are associated with strong advection from the tropics, whereas indicators of the cold La Niña phase reflect weak northward transport. We used three indicators for El Niño: one atmospheric, one oceanographic, and one multivariate indicator that includes both oceanographic and atmospheric variables. The Southern Oscillation Index (SOI), calculated as monthly fluctuations in sea level pressure between the Tahiti Low and Darwin, Australia High, was used as an indicator of the atmospheric drivers of ENSO. Prolonged negative values signify El Niño episodes while sustained positive values are associated with La Niña episodes. To present the SOI in phase with other variables, we reversed the sign of this indicator, such that positive values reflect El Niño and negative values reflect La Niña. Data were calculated by the Climate Analysis Section, National Center for Atmospheric Research, and were obtained from http://www.cgd.ucar.edu/cas/catalog/climind/SOI.signal.ascii. The Oceanic Nino Index (ONI), a 3-month running mean of SST anomalies in the region 5°N-5°S, 120-170°W (Nino3.4), was used as an oceanographic manifestation of the ENSO cycle. The ONI is computed by the NOAA National Weather Service, Center for Climate Prediction. Data were obtained from http://www.cpc.ncep.noaa.gov/products/analysis_monitoring/ensostuff/ensoyears.shtml. The Multivariate ENSO Index (MEI), based on six observed variables over the tropical Pacific, was used as an indicator of the tropical oceanographic manifestation of the ENSO cycle (Wolter and Timlin, 1993). Negative values of the MEI represent the cold ENSO phase (La Niña), while positive MEI values represent the warm ENSO phase (El Niño). Data were obtained from NOAA's Earth System Research Laboratory at http://www.esrl.noaa.gov/psd/enso/mei/table.html.

2.1.2 Indicators of Transport from the Extra-Tropics

We selected the North Pacific Index (NPI), the area-weighted sea level pressure over the region 30°N-65°N, 160°E-140°W, as our atmospheric driver of transport from the North Pacific to the California Current. Data were calculated by the Climate Analysis Section, National Center for Atmospheric Research and were downloaded from http://www.cgd.ucar.edu/cas/jhurrell/indices.data.html#npmon. This variable provides an index of the strength and positioning of the Aleutian Low Pressure system, which in turn is expressed in large-scale ocean conditions in the North Pacific reflected in the Pacific Decadal Oscillation (PDO) and North Pacific Gyre Oscillation Index (NPGO). The NPGO index was downloaded from http://eros.eas.gatech.edu/npgo/data/NPGO.txt and emerges as the second EOF of Northeast Pacific sea-surface height anomalies (Di Lorenzo et al., 2008). Positive values also indicate a strong North Pacific gyre and advective transport from the north, whereas negative values indicate a weak gyre and decreased southward transport (Hooff and Peterson, 2006; Keister et al., 2011). We also used the PDO index, developed by Zhang et al. (1997), as an oceanographic index of sub-arctic influences on the CCE. Data were downloaded from the Joint Institute for the Study of the Atmosphere and Ocean at the University of Washington. Methods and details of computation are available at http://jisao.washington.edu/pdo/PDO.latest. The PDO reflects SST for the entire North Pacific, including the CCE, at locations > 20°N. Positive values of the PDO indicate warm SST along the eastern north Pacific and cool SST over the central and western north Pacific.

2.1.3 Indicators of Regional Upwelling

The Northern Oscillation Index (NOI) provides an index of the strength and positioning of the North Pacific High pressure system which, with the Continental Thermal Low, drives the winds that cause upwelling in north-central California (Schwing et al., 2002). The NOI is calculated by the Pacific Fisheries Environmental Laboratory, NOAA, based on monthly fluctuations in the sea level pressure difference between the North Pacific High and Darwin, Australia, Low thus also including variability from the tropics. NOI data were downloaded from http://www.pfeg.noaa.gov/products/PFEL/modeled/indices/NOIx/noix_download.html. The timing and amplitude of upwelling is proxied by the Bakun Upwelling Index (UI), calculated by NOAA's Environmental Research Division, from estimates of the magnitude of the offshore component of the Ekman transport driven by wind stress (Schwing et al., 1996, 2006; Bograd et al., 2009). Positive values indicate upwelling while negative values indicate downwelling. Methods and details of computation are available from http://www.pfeg.noaa.gov/products/PFEL/modeled/indices/upwelling/NA/how_computed.html. For this report we used UI indicators from 36°N 122°W and 39°N 125°W.

2.1.4 Indicators of Local Current Flows

Flow in the California Current in the sub-arctic region of the Northeast Pacific was calculated by Howard Freeland of Fisheries and Oceans Canada using data collected by Argo profiling floats (http://www.argo.net/; Freeland and Cummins, 2005). Positive values indicate stronger flows whereas negative values indicate weaker flows. Surface flow data were also collected by High-Frequency (HF) Radar (Barrick and Lipa, 1979) off of Point Reyes, California, in conjunction with the Coastal Ocean Currents Monitoring Program (COCMP; Halle and Largier, 2011), and a surface current flow index was produced. Radial data from two standard range stations, BML1 (located at Bodega Bay) and PREY (located at South Beach, Point Reyes) were combined using standard CODAR data processing methods (Kaplan et al., 2005). The Point Reyes flow index is defined in terms of four cells, each measuring approximately 14.6 km x 18.5 km (270 km^2) starting at the coast and extending approximately 51.2 km out to sea from Point Reyes, including the area around Cordell Bank. The cell boundaries are defined by lines of longitude and latitude spaced at 10-minute intervals between 123°0'W 38°0'N and 123°40'W 38°10'N. Within each cell, an hourly-based total vector file was processed to calculate daily and monthly average U (westward) and V (southward) current values from all the vectors located within each cell. Here, we focus on the V component. Negative values indicate current flow in a southward direction, but to put this variable in phase with the others we reversed the sign, therefore positive values indicate stronger surface flows to the south.

2.1.5 Indicators of Local Atmospheric and Hydrographic Conditions

We used alongshore wind stress as an index of upwelling-favorable winds in the region. García-Reyes and Largier (2010, 2012) calculated this variable based on wind speed and direction measured at NOAA buoys at Point Arena (39.2°N 124.0°W), Bodega Bay (38.2°N 123.3°W), San Francisco (37.8°N 122.8°W) and Half Moon Bay (37.4°N 122.9°W). Negative values indicate wind stress in an upwelling-favorable equatorial direction, but for better interpretation of this variable we reversed the sign to make it in phase with other indicators. Details of the methodology can be found in García-Reyes and Largier (2010, 2012). Sea level measurements (mm), compiled by the National Water Level Observation Network (NWLON), were obtained from the Center for Operational Oceanographic Products and Services (CO-OPS; NOS, 2008). We used monthly data, which represent an average of daily values, from the San Francisco (37.8°N 122.5°W), Crescent City (41.4°N 124.1°W), and South Beach (41.5°N 124.1°W) sea level gauges. Methods and data were downloaded from the University of Hawaii Sea Level Center (http://uhslc.soest.hawaii.edu/). Local sea level also indexes upwelling and transport. Sea surface temperature data (SST; °C) were collected from the Farallon Islands shore station (37.7°N 123°W), NOAA buoys (Point Arena (39.2°N 124.0°W), Bodega Bay (38.2°N 123.3°W), San Francisco (37.8°N 122.8°W), Half Moon Bay (37.4°N 122.9°W) and Monterey Bay (36.8°N 122.4°W)), and the Bodega Ocean Observing Node (BOON) program at the UC Davis Bodega Marine Lab (38.3°N 123.1°W). Methods and data for the Farallon Islands shore station are available from http://shorestation.ucsd.edu/methods/index_methods.html. Buoy data were downloaded from the National Data Buoy Center (http://www.ndbc.noaa.gov/) and Bodega Marine Lab SST data were downloaded from http://bml.ucdavis.edu/boon/data_seatemp.html. Salinity data (psu) from the Farallon Islands (37.7°N 123°W) and the Bodega Marine Lab (38.3°N 123.1°W) were also compiled. Data were downloaded from ftp://ftp.iod.ucsd.edu/shore/active_data/farallon/salinity/ and http://bml.ucdavis.edu/boon/data_salinity.html, respectively. Air temperature (°C) was measured at the Bodega Marine Lab (BML; 38.3°N 123.1°W) in a weather box 40 m from the coastal bluff. Data were obtained from http://bml.ucdavis.edu/boon/data_airtemp.html. Daily temperatures were averaged to monthly values for analysis. Lastly, precipitation (cm) and air temperature (°C) data were downloaded from the National Climate Data Center, NOAA (http://cdo.ncdc.noaa.gov/pls/plclimprod/somdmain.somdwrapper?datasetabbv=DS3220&countryabbv=&georegionabbv=&forceoutside) for the sites Fort Ross (38.5°N 123.3°W), San Francisco (37.7°N 122.5°W), Pacifica (37.6°N 122.5°W), and Half Moon Bay (37.5°N 122.5°W).

2.1.6 Lower Trophic Level Indicator

We used a data set of regional satellite-derived chlorophyll-a (chl-a) combined from multiple sources into a consistent time series of spatial data sets (images) to achieve the longest temporal coverage possible. Methods for the compilation of this data set are described by Kahru et al. (2012). Briefly, long term measurements of phytoplankton biomass, proxied by estimates of chlorophyll-a, can be obtained *in situ* and by ocean color satellites. However, as the life-span of a single satellite sensor is limited, seamlessly merging ocean color observation data from multiple satellite sensors that have different optical bands, sensitivities, noise patterns and overpass times (Maritorena and Siegel, 2005) into a single unified time series remains a major challenge (Gregg et al., 2009). For this study, Kahru et al. consolidated outputs from four major ocean color sensors and created new algorithms to make output from these sensors compatible with each other and with *in situ* chlorophyll-a data collected in the region. To accomplish this task, Kahru et al. matched values from full-resolution Level-2 satellite data (OCTS, SeaWiFS, MODIS-Aqua, and MERIS) with a data set of 10,050 near-surface *in situ* chlorophyll-a measurements taken from ships over the period 1996 through 2010. All satellite sensors showed strong positive correlations with *in situ* data with the coefficient of determination (r^2) for the spatial matches ranging from 0.791 (SeaWiFS) to 0.864 (OCTS). At the same time, significant biases were observed between *in situ* and satellite data. Kahru et al. minimized the differences and created algorithms that were consistent with both *in situ* and satellite-based sensors. The optimized algorithms were then applied to the daily Level-3 remote sensing data sets of the four sensors and merged into unified daily chlorophyll-a data sets. The merged daily data were then composited into monthly data sets. Chlorophyll-a concentration is log-normally distributed. To account for this, we log transformed monthly chlorophyll-a data before calculating a monthly average and subtracting the monthly average from each log transformed monthly value to create anomalies.

2.1.7 Upper Trophic Level Indicator

Reproductive success for the seabirds common murre (*Uria aalge*), pigeon guillemot (*Cepphus columba*), Cassin's auklet (*Ptychoramphus aleuticus*), and Brandt's cormorant (*Phalacrocorax penicillatus*) was studied at Southeast Farallon Island, California, 37.7°N 123°W, by PRBO Conservation Science. Reproductive success was the number of offspring departing the colony per breeding pair per year (Sydeman et al., 2001). Data were available for 1971-2007 for all species except common murre, which were available for 1972-2007. Seabird data were de-trended using quadratic regression and the residuals were saved for further analysis.

2.2 Data Processing and Statistical Analyses

Monthly measurements of environmental conditions were expressed as anomalies (monthly value – long-term monthly average; based on full length of time series, see Table 1). To integrate measurements of each variable from different sites (i.e., seven sites of measures of SST, four locations of wind stress measurements) we used empirical orthogonal function/principal component analysis (PCA; Legendre and Legendre, 1998). The unrotated first principal component (PC1) for each variable type was extracted and retained for further analysis and evaluation. To test for trends in univariate indicators, we conducted Spearman rank correlations on each variable over time for each measurement site as well as for variable type PC1s. To test for relationships between variables, we used Spearman rank cross-correlations. To create seasonal MOCI, we used monthly values averaged across months for the following seasons: winter (January-March), spring (April-June), summer (July-September) and fall (October-December). Residuals of seasonal averages were calculated and used in a PCA conducted on all oceanic and atmospheric variables except surface flow, by season, for the years 1990-2010. The unrotated first principal component (MOCI1) for each season was extracted and retained. The seasonal MOCI described above used the full suite of climate variables, from large-scale indices to local-scale measurements. We also generated two additional sub-groups of seasonal MOCI using PCA from (1) only the large-scale climate indices and (2) only the regional-local measurements. Subsequently, we cross-correlated these sub-groups with our original MOCI of the full suite of large-scale as well as local climate variables to investigate similarities and differences between these approaches. As we were primarily interested in environmental conditions leading up to the growing season each year (~March-August), we examined the cross-correlations of MOCI and the sub-groups for fall of $year_{x-1}$ and winter, spring, and summer of $year_x$. Last, we correlated the full-suite seasonal MOCI with the de-trended biological indicators. For chlorophyll-a, we created an annual time series by averaging monthly residuals from October to September. We used fall MOCI of the previous year and winter, spring, and summer MOCI of the concurrent year to test for temporal associations. The seabird residual data were synthesized using PCA and the first principal component ($PC1_{seabirds}$) was saved for analyses. Seabird species residual data and $PC1_{seabirds}$ were tested against seasonal MOCI of the same year.

3. Results

3.1 Status and Trends in Basin-Scale Indicators

Results of spearman rank correlation tests for data trends are shown in Table 2. The SOI, MEI, and ONI showed negative trends (Fig. 1), indicating a decrease in the frequency and amplitude of El Niño events. 2010 values for the SOI and MEI were particularly anomalous (almost 2x standard deviation), indicating a strong La Niña event in that year. However, this followed a moderate El Niño from mid-2009 through early 2010. For extra-tropical indices, the NPI showed no trend (Fig. 2a) while the PDO decreased (indicating cooling of the eastern Pacific, Fig. 2b). The NPGO increased (indicating greater gyre transport) with a distinct step from negative to mostly positive values in early 1998 (Fig. 2c) and showed a strong period of transport from early 1999 to early 2003, which corresponds to negative values of the PDO during the same time period. The NPGO has been largely positive since early 2010, corresponding to a negative PDO. Changes in the NPGO and PDO during the El Niño of 2009 were not particularly noteworthy (i.e., well within 1 s.d. of the mean).

3.2 Status and Trends in Regional Upwelling Indicators

The NOI increased in the study period though the overall rate of change was small (Table 2, Fig. 3a). The NOI was strongly negative (indicating a weak North Pacific High) in early 2010, corresponding to the 2009-2010 El Niño, but rebounded to normal levels later in the year. The NOI was particularly high from mid-2007 to early 2009, and was low but not outside 1 s.d. of the mean from late 2002 through 2006. Similar to the NOI, the UI at 36°N and 39°N had a slight, but significantly positive trend (Table 2, Fig. 3b). Strong negative values in late 2009 indicate downwelling during the 2009-2010 El Niño, and the highest values were observed from 1999 through 2002.

3.3 Status and Trends in Regional and Local-Scale Current Indicators

There was no trend in the flow of the California Current based on Argo measurements, 2002-2010 (Table 2, Fig. 4a). An anomalously low flow rate was detected, however, for mid-late 2004 and early-mid 2010. The largest flow was observed from mid 2007 to late 2008. Local flow of surface currents off Point Reyes were generally in the positive (increasing) direction (Fig. 4b) though only for cell 2 was the trend significant (Table 2). Local surface currents were highly variable within and between months and years. A peak in the surface flow off Point Reyes was observed in 2004 (opposite to flow in the California Current), with another increase in 2007-2008 (corresponding to high California Current flows).

3.4 Status and Trends in Regional Wind and Hydrographic Indicators

Clear trends were observed for wind stress and SST (Table 2, Fig. 5a,b). Wind stress increased significantly at all sites and was particularly strong in 2008 but decreased in 2009. SST decreased significantly at 4 of 7 locations over the 21-year period and was particularly low for the period 2007-2010. The only significant change in sea level, however, was decreasing sea level at Crescent City (Table 2, Fig. 5c). Sea level was elevated in late 2009, corresponding to the El Niño event at that time, but has since decreased. There were no significant trends for salinity (Fig. 5d). Corresponding to the cold SST, salinity in recent years has also been elevated but decreased from 2007-2010 and was not outside average values in most of 2009 and 2010.

3.5 Status and Trends in Regional Air Temperature and Precipitation Indicators

Air temperature represented by five sites showed a decreasing trend (Table 2, Fig. 6a) with the exception of Pacifica where the trend was positive and non-significant. Air temperature was generally low from 2008-2010. There was no overall trend for precipitation (Fig. 6b).

3.6 Variable-Specific Multivariate Indicators

Within key climate variable types, creating linear combinations of sites using PCA was supported and interpretable. Eigenvalues for the first principal component (PC1) were >3 for surface flow at Point Reyes, wind stress, SST, air temperature and precipitation (Table 3a). Within each of these variables, loadings for different sites were similar (Table 3b). For example, loadings for SST, which include data from seven sites, ranged from 0.338 (Monterey Bay) to 0.407 (Farallon Islands). Similarly, loadings for wind stress for four sites ranged from 0.465 (San Francisco) to 0.514 (Half Moon Bay). This reveals strong covariance between sites as well as similar contributions from each site to each multivariate index, thus justifying our approach. Trends in multivariate indices for upwelling, wind stress, and SST confirmed the pattern seen in univariate analyses of increasing NOI, increasing upwelling-favorable wind stress, and decreasing SST in the region (Table 2).

3.7 Correlations Among Physical Environmental Indicators

Correlations between environmental indicators are shown in Table 4. These correlations are based on monthly data and are therefore highly autocorrelated. Due to this concern, we did not attempt to assign statistical significance to these correlations, but instead highlight associations with rho > 0.5. Not surprisingly, the three sub-tropical indices (SOI, MEI, ONI) were well related to one another. The NOI was related to the upwelling index, surface flow at Point Reyes, wind stress, SST, and sea level. SST and salinity were negatively correlated, while SST and air temperature were positively associated. Notably, at the rho > 0.5 level, the NPI, NPGO, and California Current flow were unrelated to any other indicators.

3.8 Development of Seasonal Multivariate Ocean-Climate Indicators (MOCI)

Due to seasonal variation, we used PCA to create linear combinations of all physical variables within seasons (Table 5). There were distinct differences in the MOCI created for winter (JFM) and spring (AMJ) versus summer (JAS) and fall (OND). The eigenvalues for winter and spring were >18 whereas summer and fall were <14; this related to greater variance explained in the first two seasons (56% and 53%, respectively) compared to the latter seasons (38% and 40%, respectively; Table 5a). The second principle components for each seasonal MOCI were balanced with eigenvalues >4, and the variance explained by each was ~13.5%. MOCI1-winter appeared to primarily be explained by a weak NOI (weak North Pacific High) and positive sea level and SST (Table 5b, Fig. 7a). We interpret MOCI1-winter as an index of wintertime atmospheric pressure and upwelling. MOCI2-winter was explained primarily by variation in precipitation (Table 5b); we therefore interpret MOCI2-winter as an indicator of local winter atmospheric conditions, including the PDO. MOCI1-spring appeared to be explained primarily by negative upwelling at 39°N and positive sea level and SST (Table 5b, Fig. 7b). Thus, we interpret MOCI1-spring as an index of PDO-driven variation in sea level and SST (high and warm). MOCI2-spring was explained primarily by variation in SOI (positive) and NPI (negative; Table 5b), as well as precipitation. MOCI1-summer appeared to be explained primarily by positive sea level, SST, and air temperature (Table 5b, Fig. 7c). We interpret MOCI1-summer as an index of temperature. MOCI2-summer was explained primarily by weak (positive) wind stress coupled with temperature and precipitation (Table 5b). Last, MOCI1-fall appeared to be related to the PDO (positive), NOI (negative), weak wind stress, and positive sea level and SST (Table 5b, Fig. 7d), reflecting weak upwelling conditions. MOCI2-fall was explained primarily by variation in SOI, MEI, and ONI (Table 5b); therefore, we interpret MOCI2-fall as an indicator of ENSO conditions.

3.9 Trends in MOCI

Trends in seasonal MOCI are depicted in Fig. 8. MOCI1-winter showed strong upwelling in 1990 and 2007-2008, and particularly weak upwelling in 1992, 1995, 1998, 2005 and 2010. The overall trend for MOCI1-winter is for more upwelling interannually. MOCI1-spring showed elevated sea level and SST in 1992, 1998, and 2005-2006, and low sea level and cold SST in 1991, 1999, 2001-2002 and 2008. The trend for MOCI1-spring is for lower sea level and SST through time. MOCI1-summer showed warming in 1997 and 2004 and cooling in 1994, 1996, 2000-2001 and 2010. The overall trend for MOCI1-summer is for ocean cooling, but this is driven largely by 2010. MOCI1-fall showed weak upwelling in 1992, 1997, and 2002, and particularly strong upwelling in 1990, 1998, 2000, and 2007. There is no overall trend in upwelling for MOCI1-fall. The full MOCI time series is shown in Fig. 9. Years generally categorized as subtropical, warm, and rainy with weak winds and upwelling are 1992-1998 and 2003-2007. The pronounced 1997-1998 ENSO shift is clearly seen. Years generally categorized as sub-arctic and cold with strong winds and upwelling are 1990-1991, 1999-2002, and 2007-2011.

3.10 Correlations between MOCI, Large-Scale Climate Indices, and Local Measurements

Seasonal sub-groups of MOCI produced from large-scale climate indices only and regional-local measurements only, and the original MOCI from all variables combined did not vary substantially from one another and were highly correlated (Table 6).

3.11 Status and Trends of Biological Indicators

Chlorophyll has increased since 1997 (Fig. 10a; n = 168, rho = 0.41, p-value < 0.001). There was no trend in reproductive success for pigeon guillemot or Cassin's auklet (Fig. 10b,c), but common murre had a negative trend (Fig. 10d; n = 36, rho = -0.29, p-value = 0.085) and Brandt's cormorant had a positive trend (Fig. 10e; n = 37, rho = 0.47, p-value = 0.003); both of these trends were eliminated using quadratic regression. $PC1_{seabirds}$ explained 65% of the variability in the reproductive success of these four species (Fig. 10f, eigenvalue = 2.61), and the loadings were largely equal between species (range = 0.45-0.53).

3.12 Correlations between Environmental and Biological Indicators

There were no significant relationships between seasonal MOCI and chlorophyll-a concentrations, but there were several correlations between seasonal MOCI and seabird variables. MOCI1-spring was significantly correlated with reproductive success of all seabird species as well as $PC1_{seabirds}$ (Table 7, Fig. 11). All relationships between seasonal MOCI and seabird reproductive success (including $PC1_{seabirds}$) were negative indicating reduced breeding success with increasing MOCI values. MOCI-spring explained 28%, 76%, 43%, and 37% of the variation in the breeding success of Cassin's auklet, common murre, pigeon guillemot, and Brandt's cormorant, respectively, and 59% of the variation in $PC1_{seabirds}$.

4. Discussion

Disentangling the effects of climate variability and fishing on coastal ecosystems is a challenge as both factors occur simultaneously and interact to affect food webs and biological populations (Link et al., 2002; Hsieh et al., 2008; Kenny et al., 2009; Kirby et al., 2009). As MPA designations are controversial, robust evaluations of the goals of MPAs in protecting and restoring ecosystems are needed. We implemented this study to aid in the interpretation and evaluation of ecological and biological changes within and outside newly established MPAs in the central California Current. Our primary goals were to design multivariate ecosystem indicators that capture the ocean-climate processes which affect a variety of marine life, and provide understanding of temporal environmental trends and variability in conditions during the two decades leading up to MPA designation.

4.1 Indicator Design and Development

To derive a description of environmental variability through time, we created seasonal, multivariate indicators of environmental conditions based on linear combinations of 16 well-known atmospheric and oceanographic indicators. In part, we modeled this work after Hemery et al. (2008) and Kenny et al. (2009), who took a similar approach to investigating coupled climate and ecosystem change in the Bay of Biscay, France, and the North Sea, respectively. Hemery et al. used 11 climate variables over four seasons (i.e., 44 variables described each year) to create their "Multivariate Ocean-Climate Index", and compared it to the major climate index of their region, the winter North Atlantic Oscillation (wNAO). Hemery et al. used SST, air temperature, precipitation, and wind variables, as we did, but they did not integrate measurements of salinity, surface currents, or sea level. We used all of these variables, as well as a variety of basin-scale atmospheric and oceanographic indices (listed above), to create season-specific Multivariate Ocean Climate Indices ("MOCI"; winter (January-March), spring (April-June), summer (July-September), and fall (October-December)). As most biological processes and populations in the California Current are dependent on seasonal variation in environmental conditions (e.g., Abraham and Sydeman, 2004; Black et al., 2010, 2011), we surmised that deriving seasonal MOCI would be the most appropriate way to examine physical – biological interactions in this region.

The seasonal MOCI time series we derived is shown in Fig. 9. By placing the seasonal values in sequence, we can verify whether these indicators reflect known transitions in environmental conditions, for example, those occurring during well-documented ENSO events in the eastern tropical Pacific. The strongest El Niño on record transitioned to one of the strongest La Niña events on record from 1997 to 1999 (Chavez et al., 1999). According to our MOCI, the 1997-98 El Niño reached its peak in summer 1997 and transitioned to La Niña during the spring and summer of 1998. This seasonality is temporally matched to physical, chemical, and biological changes in the tropical Pacific and central California (Chavez et al., 2002). Similarly, a weaker, though still significant transition to an El Niño event occurred from 1991 to 1992. Our seasonal MOCI indicate that this transition occurred during from winter 1991 through spring/summer 1991 and peaked in winter/spring 1992. This transitional period also matched reported changes in biogeochemical attributes of the tropical Pacific (Barber et al., 1996) and central California (Chavez, 1996) at that time. More recently, a modest El Niño occurred with the peak observed in our seasonal MOCI in winter 2010 (MEI; http://www.esrl.noaa.gov/psd/enso/mei/table.html). That MOCI match the timing of major and well-known basin-scale oceanographic transitions provides confidence that the environmental measurements selected, as well as statistical procedures used, result in MOCI that accurately represent the environmental conditions in the region.

4.2 Trends in Environmental Conditions

The state of a marine ecosystem is a function of the forces acting upon it at various temporal and spatial scales. To assess trends in environmental conditions for the north-central California coastal region, we summarized indicators for the period 1990-2010 and selected basin-, regional-, and local-scale indicators. We selected 1990 as our cutoff due to a putative "regime shift" in environmental conditions and ecosystem status that occurred at that time (Hare and Mantua, 2000; Sydeman et al., 2001). Since 1990, the primary trend in the environment of north-central coastal California can be summarized as follows: (1) a general weakening of sub-tropical influences on the system, illustrated by declining trends in the SOI, MEI, and ONI, (2) a general strengthening of sub-arctic influences, shown by cooling of the PDO and increases in the NPGO, and (3) increasing regional-scale upwelling, documented by a stronger NOI and UI at both 36°N and 39°N. We found no change in currents on either the large- (California Current flow) or local- (surface flow at Point Reyes) scale, probably because the time series for these variables were too short (2002-2010), although flow rates were generally positive as would have been expected under generally increasing sub-arctic influences. Upwelling intensification over the period was supported by observations of significantly increasing wind stress (4 of 4 buoys) and decreasing SST (4 of 7 buoys). PC1 values of wind stress and SST reflective of the entire region confirmed these patterns of change. Interestingly, despite decreasing SST, we did not observe trends in salinity or sea level. Three of five sites showed decreasing air temperature which may be related to changes in ocean temperature. In short, changes in sub-arctic influences, particularly the NPGO, and regional upwelling and ocean temperature have made the environment more temperate in nature.

4.3 Relationships between Indicators

Correlations between indicators (Table 4) confirm that three main factors appear to affect environmental conditions in the marine environment of north-central California. Highlights of robust correlations (rho > 0.5) show clusters of associations amongst ENSO-related variables (MEI, SOI, ONI) as well as their relationships to the PDO and NOI. The ENSO indicators were related to sea level and SST, but not at rho > 0.5. PDO-related associations were strong with sea level and SST as well as air temperature. The correlations between PDO and SST and sea level were positive, indicating a possible mechanistic connection between PDO and transport (indicated by sea level); SST and sea level were also strongly connected. The last cluster of correlations was associated with the NOI, including positive associations with surface flow and wind stress (indicative of upwelling) and negative associations with SST and sea level. The NOI-related cluster apparently reflects regional upwelling and local conditions. Salinity was negatively correlated with sea level and SST, as expected if sea level and SST are driven by upwelling. These clusters of associations suggest that models of physical-biological interactions could be well represented by no less than three basin-scale indicators, one for influence from the sub-tropics (MEI), one for influence from the sub-arctic (PDO), and one for upwelling (NOI). Models of physical-biological interactions at the regional or local scale would be well represented by at least one indicator, and we would suggest sea level for this purpose as it integrates all large-scale factors. Moreover, the strongest correlations we found were between sea level and the NOI (rho = -0.76) and sea level and SST (rho = 0.70). As previously suggested (Sydeman and Thompson, 2010), sea level is perhaps the best univariate indicator available for use in environmental and ecosystem assessments. Sea level was well correlated with our seasonal MOCI (Table 5).

4.4 Environmental Conditions Immediately Preceding MPA Establishment

Seasonal MOCI indicate substantial transitions and variability in the years leading up to MPA establishment along the central California coast in 2007 and north-central region in 2010 (Fig. 9). The years 2004-2006 (time preceding establishment of MPA in the NCC) were characterized by poor upwelling and generally warm conditions. The year 2008 was characterized by strong upwelling and cold SST in the winter and especially spring, which transitioned to "normal" conditions (within 1 s.d. of the average PC value) in summer and fall and continued through 2009. Winter 2010 was characterized by strong El Niño conditions, comparable to winter 1998, however, this event was relatively short-lived and by summer 2010 La Niña conditions with strong upwelling and low SST prevailed. Bjorkstedt et al. (2010) describe similar transitions in the entire CCE in 2009 and 2010. By fall 2010, conditions were within normal bounds.

4.5 Linking Environmental and Biological Indicators

As noted above, MOCI reflected well-documented environmental transitions and variability, and we are therefore confident that we selected and processed appropriate variables using multivariate procedures. However, it is clear that patterns of variability of a lower (chl-a) trophic level indicator do not match the patterns of variability in MOCI, neither seasonally nor from an interannual perspective (Fig. 10a). We found an increasing chl-a trend which may be related to positive trends in increasing wind stress (and decreasing SST; Table 2; Wilkerson et al., 2006), but found no correlations between seasonal MOCI and de-trended chl-a abundance, indicating no associations on the interannual time scale. Moreover, a peak in chl-a was observed in the 2004-2006 period when MOCI generally indicated warm conditions with weak upwelling. Measuring bulk chl-a does not provide information on phytoplankton community composition, which may explain why correlations with MOCI were elusive since phytoplankton species respond differently to transport, upwelling, and variation in local hydrographic conditions (Chavez et al., 2011). In support of this idea, the seabird indicators based on productivity of individual species were strongly associated with seasonal MOCI, with spring in particular explaining a significant proportion of the variability in species-specific and combined seabird breeding success. Seabird breeding success in itself is an integration of a several parameters including the number of eggs produced per nest (clutch size), the proportion of eggs hatched, and the proportion of hatched chicks raised to independence (for interannual variation in these parameters see Sydeman et al., 2001). Seabird breeding success has been presented previously as an indicator of prey abundance (Cairns, 1987; Piatt et al., 2007), specifically mesozooplankton (e.g., krill) and small forage fish used for offspring production (Sydeman et al., 2013). Therefore, the strong connection between seabird breeding success and spring MOCI suggests that the MOCI may also be an indicator of the coastal food webs that seabirds are dependent upon. More importantly, this provides support for our approach in both designing and implementing MOCI, and for potential application in assessing biotic changes in MPAs. The seabird correlations also support our contention that the lack of correlation with bulk chl-a may be due to poor information content about which species of phytoplankton are represented in the chl-a values obtained via satellite remote-sensing.

5. Conclusion

We designed and implemented multivariate indicators of ocean climate (MOCI) for the north-central study region based on processes known to affect populations and ecosystem dynamics there (transport from the south and north and regional upwelling). The seasonal MOCI represented environmental variability well and show promise for understanding physical-biological interactions in the system. MOCI can be used to put biological findings in the context of broader environmental variability.

6. Acknowledgements

For data contributions to this project, we thank John Largier and Marcel Losekoot (Bodega Marine Lab) for providing information of surface currents, Jim Johnstone (JISAO, University of Washington) for providing data on air temperature and precipitation, Howard Freeland (Fisheries and Oceans Canada) for providing data on California Current flow rates from the Argo array, and PRBO for data on seabird breeding success. We thank the State of California's MPA Monitoring Enterprise, the Ocean Science Trust, California Sea Grant, and the National Science Foundation (California Current Ecosystem Long-term Ecological Research program) for financial support.

7. Literature Cited

Abraham, C.L., Sydeman, W.J., 2004. Ocean climate, euphausiids and auklet nesting: inter-annual trends and variation in phenology, diet and growth of a planktivorous seabird, *Ptychoramphus aleuticus*. Marine Ecology Progress Series 274, 235-250.

Ainley, D.G., Sydeman, W.J., Norton, J., 1995. Upper trophic level predators indicate interannual negative and positive anomalies in the California Current food web. Marine Ecology Progress Series 118, 69-79.

Barber, R.T., Sanderson, M.P., Lindley, S.T., Chai, F., Newton, J., Trees, C.C., Foley, D.G., Chavez, F.P., 1996. Primary productivity and its regulation in the equatorial Pacific during and following the 1991-1992 El Niño. Deep-Sea Research Part II 43, 933-969.

Barrick, D.E., Lipa, B.J., 1979. A compact transportable HF radar system for directional coastal wave field measurements. In Earle, M.D., Malahoff, A., (Eds.), Ocean Wave Climate. Plenum Press, Plenum, New York, pp. 153-201

Bjorkstedt, E.P., Goericke, R., McClatchie, S., Weber, E., Watson, W., Lo, N., Peterson, B., Emmett, B., Peterson, J., Durazo, R., Gaxiola-Castro, G., Chavez, F., Pennington, J.T., Collins, C.A., Field, J., Ralston, S., Sakuma, K., Bograd, S.J., Schwing, F.B., Xue, Y., Sydeman, W.J., Thompson, S.A., Santora, J.A., Largier, J., Halle, C., Morgan, S., Kim, S.Y., Merkens, K.P.B., Hildebrand, J.A., Munger, L.M., 2010. State of the California Current 2009-2010: Regional variation persists through transition from La Niña to El Niño (and back?). California Cooperative Oceanic Fisheries Investigations Report 51, 39-69.

Black, B.A., Schroeder, I.D., Sydeman, W.J., Bograd, S.J., Lawson, P.W., 2010. Wintertime ocean conditions synchronize rockfish growth and seabird reproduction in the central California Current ecosystem. Canadian Journal of Fisheries and Aquatic Sciences 67, 1149-1158.

Black, B.A., Schroeder, I.D., Sydeman, W.J., Bograd, S.J., Wells, B.K., Schwing, F.B., 2011. Winter and summer upwelling modes and their relevance to climate impacts and ecological response in the California Current Ecosystem. Global Change Biology 17, 2536-2545.

Bograd, S.J., Schroeder, I., Sarkar, N., Qiu, X.M., Sydeman, W.J., Schwing, F.B., 2009. Phenology of coastal upwelling in the California Current. Geophysical Research Letters 36, L01602.

Bond, N.A., Overland, J.E., Spillane, M., Stabeno, P.J., 2003. Recent shifts in the state of the North Pacific. Geophysical Research Letters 30, 2183.

Cairns, D.K., 1987. Seabirds as indicators of marine food supplies. Biological Oceanography 5, 261-271.

Carr, M.H., Woodson, C.B., Cheriton, O.M., Malone, D., McManus, M.A., Raimondi, P.T., 2011. Knowledge through partnerships: integrating marine protected area monitoring and ocean observing systems. Frontiers in Ecology and the Environment 9, 342-350.

Chavez, F.P., 1996. Forcing and biological impact of onset of the 1992 El Niño in central California. Geophysical Research Letters 23, 265-268.

Chavez, F.P., Strutton, P.G., Friederich, G.E., Feely, R.A., Feldman, G.C., Foley, D.G., McPhaden, M.J., 1999. Biological and chemical response of the Equatorial Pacific Ocean to the 1997-98 El Niño. Science 286, 2126-2131.
Chavez, F.P., Pennington, J.T., Castro, C.G., Ryan, J.P., Michisaki, R.P., Schlining, B., Walz, P., Buck, K.R., McFadyen, A., Collins, C.A., 2002. Biological and chemical consequences of the 1997-1998 El Niño in central California waters. Progress in Oceanography 54, 205-232.
Chavez, F.P., Messie, M., Pennington, J.T., 2011. Marine primary production in relation to climate variability and change. Annual Review of Marine Science 3, 227-260.
Checkley, D.M., Barth, J.A., 2009. Patterns and processes in the California Current System. Progress in Oceanography 83, 49-64.
Chelton, D.B., Bernal, P.A., McGowan, J.A., 1982. Large-scale interannual physical and biological interactions in the California Current. Journal of Marine Research 40, 1095-1125.
Cury, P.M., Shin, Y.J., Planque, B., Durant, J.M., Fromentin, J.M., Kramer-Schadt, S., Stenseth, N.C., Travers, M., Grimm, V., 2008. Ecosystem oceanography for global change in fisheries. Trends in Ecology & Evolution 23, 338-346.
Di Lorenzo, E., Schneider, N., Cobb, K.M., Franks, P.J.S., Chhak, K., Miller, A.J., McWilliams, J.C., Bograd, S.J., Arango, H., Curchitser, E., Powell, T.M., Riviere, P., 2008. North Pacific Gyre Oscillation links ocean climate and ecosystem change. Geophysical Research Letters 35, L08607.
Freeland, H.J., Cummins, P.F., 2005. Argo: A new tool for environmental monitoring and assessment of the world's oceans, an example from the NE Pacific. Progress in Oceanography 64, 31-44.
García-Reyes, M., Largier, J., 2010. Observations of increased wind-driven coastal upwelling off central California. Journal of Geophysical Research 115, C04011.
García-Reyes, M., Largier, J.L., 2012. Seasonality of coastal upwelling off central and northern California: New insights, including temporal and spatial variability. Journal of Geophysical Research 117, C03028.
Gregg, W.W., Casey, N.W., O'Reilly, J.E., Esaias, W.E., 2009. An empirical approach to ocean color data: Reducing bias and the need for post-launch radiometric re-calibration. Remote Sensing of Environment 113, 1598-1612.
GRL Special Section. 2006. Warm ocean conditions in the California Current in spring/summer 2005: Causes and consequences. Geophysical Research Letters 33(22).
Halle, C.M., Largier, J.L., 2011. Surface circulation downstream of the Point Arena upwelling center. Continental Shelf Research 31, 1260-1272.
Hare, S.R., Mantua, N.J., 2000. Empirical evidence for North Pacific regime shifts in 1977 and 1989. Progress in Oceanography 47, 103-145.
Hemery, G., D'Amico, F.D., Castege, I., Dupont, B., D'Elbee, J., Lalanne, Y., Mouches, C., 2008. Detecting the impact of oceano-climatic changes on marine ecosystems using a multivariate index: The case of the Bay of Biscay (North Atlantic-European Ocean). Global Change Biology 14, 27-38.
Hjort, J., 1914. Fluctuations in the great fisheries of northern Europe viewed in the light of biological research. Rapport et Proces-verbaux des Reunions, Conseil International pour l'Exploration de la Mer 20, 1-228.

Hooff, R.C., Peterson, W.T., 2006. Copepod biodiversity as an indicator of changes in ocean and climate conditions of the northern California current ecosystem. Limnology and Oceanography 51, 2607-2620.

Hsieh, C.H., Reiss, C.S., Hewitt, R.P., Sugihara, G., 2008. Spatial analysis shows that fishing enhances the climatic sensitivity of marine fishes. Canadian Journal of Fisheries and Aquatic Sciences 65, 947-961.

Huyer, A., 1983. Coastal upwelling in the California Current System. Progress in Oceanography 12, 259-284.

Kahru, M., Kudela, R.M., Manzano-Sarabia, M., Mitchell, B.G., 2012. Trends in the surface chlorophyll of the California Current: Merging data from multiple ocean color satellites. Deep-Sea Research Part II, 77–80, 89–98.

Kaplan, D.M., Largier, J., Botsford, L.W., 2005. HF radar observations of surface circulation off Bodega Bay (Northern California, USA). Journal of Geophysical Research - Oceans 110, C10020.

Keister, J.E., Di Lorenzo, E., Morgan, C.A., Combes, V., Peterson, W.T., 2011. Zooplankton species composition is linked to ocean transport in the Northern California Current. Global Change Biology 17, 2498-2511.

Kenny, A.J., Skjoldal, H.R., Engelhard, G.H., Kershaw, P.J., Reid, J.B., 2009. An integrated approach for assessing the relative significance of human pressures and environmental forcing on the status of Large Marine Ecosystems. Progress in Oceanography 81, 132-148.

Kirby, R.R., Beaugrand, G., Lindley, J.A., 2009. Synergistic effects of climate and fishing in a marine ecosystem. Ecosystems 12, 548-561.

Legendre, P., Legendre, L., 1998. Numerical Ecology. Elsevier, Amsterdam.

Lenarz, W.H., Ventresca, D.A., Graham, W.M., Schwing, F.B., Chavez, F., 1995. Explorations of El Niño events and associated biological population dynamics off central California. California Cooperative Oceanic Fisheries Investigations Reports 36, 106-119.

Levin, P.S., Fogarty, M.J., Murawski, S.A., Fluharty, D., 2009. Integrated Ecosystem Assessments: Developing the scientific basis for ecosystem-based management of the ocean. PLoS Biology 7, 23-28.

Link, J.S., Brodziak, J.K.T., Edwards, S.F., Overholtz, W.J., Mountain, D., Jossi, J.W., Smith, T.D., Fogarty, M.J., 2002. Marine ecosystem assessment in a fisheries management context. Canadian Journal of Fisheries and Aquatic Sciences 59, 1429-1440.

Mackas, D.L., Batten, S., Trudel, M., 2007. Effects on zooplankton of a warmer ocean: Recent evidence from the Northeast Pacific. Progress in Oceanography 75, 223-252.

Mantua, N.J., Hare, S.R., Zhang, Y., Wallace, J.M., Francis, R.C., 1997. A Pacific interdecadal climate oscillation with impacts on salmon production. Bulletin of the American Meteorological Society 78, 1069-1079.

Maritorena, S., Siegel, D.A., 2005. Consistent merging of satellite ocean color data sets using a bio-optical model. Remote Sensing of Environment 94, 429-440.

McGowan, J.A., Bograd, S.J., Lynn, R.J., Miller, A.J., 2003. The biological response to the 1977 regime shift in the California Current. Deep-Sea Research Part II - Topical Studies in Oceanography 50, 2567-2582.

McPhaden, M.J., Zebiak, S.E., Glantz, M.H., 2006. ENSO as an integrating concept in Earth science. Science 314, 1740-1745.

NOS 2008. CO-OPS specifications and deliverables for installation, operation, and removal of water level stations. Requirements and Developmental Division, Center for Operational Oceanographic Products and Services, National Ocean Service, NOAA.

Peña, M.A., Bograd, S.J., 2007. Time series of the northeast Pacific. Progress in Oceanography 75, 115-119.

Peterson, W.T., Schwing, F.B., 2003. A new climate regime in Northeast Pacific ecosystems. Geophysical Research Letters 30, 1896.

Piatt, J.F., Harding, A.M.A., Shultz, M., Speckman, S.G., Van Pelt, T.I., Drew, G.S., Kettle, A.B., 2007. Seabirds as indicators of marine food supplies: Cairns revisited. Marine Ecology Progress Series 352, 221-234.

Ralston, S., Sakuma, K.M., Field, J.C., 2013. Interannual variation in pelagic juvenile rockfish (*Sebastes* spp.) abundance – going with the flow. Fisheries Oceanography, in press. doi:10.1111/fog.12022.

Rice, J.C., Rochet, M.J., 2005. A framework for selecting a suite of indicators for fisheries management. ICES Journal of Marine Science 62, 516-527.

Schwing, F.B., O'Farrell, M., Steger, J.M., Baltz, K., 1996. Coastal upwelling indices, west coast of North America, 1946-1995. NOAA-TM-NMFS-SWFSC-231.

Schwing, F.B., Murphree, T., deWitt, L., Green, P.M., 2002. The evolution of oceanic and atmospheric anomalies in the northeast Pacific during the El Niño and La Niña events of 1995-2001. Progress in Oceanography 54, 459-491.

Schwing, F.B., Bond, N.A., Bograd, S.J., Mitchell, T., Alexander, M.A., Mantua, N., 2006. Delayed coastal upwelling along the US West Coast in 2005: A historical perspective. Geophysical Research Letters 33, L22S01.

Sydeman, W.J., Thompson, S.A., 2010. The California Current Integrated Ecosystem Assessment (IEA), Module II: Trends and variability in climate-ecosystem state. Report to NOAA, SWFSC, Environmental Research Division. Pacific Grove, California.

Sydeman, W.J., Hester, M., Thayer, J.A., Gress, F., Martin, P., Buffa, J., 2001. Climate change, reproductive performance and diet composition of marine birds in the southern California Current System, 1967-1997. Progress in Oceanography 49, 309-329.

Sydeman, W.J., Bradley, R.W., Warzybok, P., Abraham, C.L., Jahncke, J., Hyrenbach, K.D., Kousky, V., Hipfner, J.M., Ohman, M.D., 2006. Planktivorous auklet *Ptychoramphus aleuticus* responses to ocean climate, 2005: Unusual atmospheric blocking? Geophysical Research Letters 33, L22S09.

Sydeman, W.J., Mills, K.L., Santora, J.A., Thompson, S.A., Bertram, D.F., Morgan, K.H., Wells, B.K., Hipfner, J.M., Wolf, S.G., 2009. Seabirds and climate in the California Current--A synthesis of change. California Cooperative Oceanic Fisheries Investigations Reports 50, 82-104.

Sydeman, W.J., Santora, J.A., Thompson, S.A., Marinovic, B., Di Lorenzo, E., 2013. Increasing variance in North Pacific climate explains unprecedented ecosystem variability off California. Global Change Biology, in press.

Thompson, S.A., Sydeman, W.J., Santora, J.A., Black, B.A., Suryan, R.M., Calambokidis, J., Peterson, W.T., Bograd, S.J., 2012. Linking predators to seasonality of upwelling: Using food web indicators and path analysis to infer trophic connections. Progress in Oceanography 101, 106-120.

Wilkerson, F.P., Lassiter, A.M., Dugdale, R.C., Marchi, A., Hogue, V.E., 2006. The phytoplankton bloom response to wind events and upwelled nutrients during the CoOP WEST study. Deep-Sea Research Part II 53, 3023-3048.

Wolter, K., Timlin, M.S., 1993. Monitoring ENSO in COADS with a seasonally adjusted principal component index. In Proceedings of the 17th Climate Diagnostics Workshop, Norman, Oklahoma, pp. 52-57.

Zhang, Y., Wallace, J.M., Battisti, D.S., 1997. ENSO-like interdecadal variability: 1900-93. Journal of Climate 10, 1004-1020.

Table 1. Data sets used. Shown for each variable is the year of the beginning of the full time series (all data sets extend through 2010) and the source for the data.

Variable Type	Variable	Beginning Year of Time Series	Data Source
Sub-tropical Climate Indices	Southern Oscillation Index	1900	Climate Analysis Section, National Center for Atmospheric Research
	Multivariate ENSO Index	1950	Earth System Research Laboratory, NOAA
	Oceanic Nino Index	1950	Center for Climate Prediction, National Weather Service, NOAA
Sub-arctic Climate Indices	North Pacific Index	1900	Climate Analysis Section, National Center for Atmospheric Research
	North Pacific Gyre Oscillation	1950	Emanuele Di Lorenzo, Georgia Institute of Technology
	Pacific Decadal Oscillation	1900	Joint Institute for the Study of the Atmosphere and Ocean, University of Washington
Upwelling	Northern Oscillation Index	1970	Pacific Fisheries Environmental Laboratory, NOAA
	Bakun Upwelling Index 36°N	1946	Environmental Research Division, NOAA
	Bakun Upwelling Index 39°N	1946	
California Current Flow	California Current	2002	Howard Freeland, Fisheries and Oceans Canada
	Point Reyes Cell 0	2001	Bodega Marine Lab, University of California Davis
	Point Reyes Cell 1	2001	
	Point Reyes Cell 2	2001	
	Point Reyes Cell 3	2001	
Wind Stress	Bodega Bay	1982	Marisol Garcia-Reyes, University of California Davis
	San Francisco	1982	
	Half Moon Bay	1982	
	Monterey Bay	1982	
Sea Level	South Beach	1967	National Water Level Observation Network, Center for Operational Oceanographic Products and Services
	Crescent City	1933	
	San Francisco	1901	
Sea Surface Temperature	Point Arena	1982	NOAA
	Bodega Marine Lab	1988	Bodega Ocean Observing Node, Bodega Marine Lab, University of California Davis
	Bodega Bay	1981	NOAA
	San Francisco	1983	
	Farallon Islands	1955	Scripps Institution of Oceanography Shore Stations Program
	Half Moon Bay	1981	NOAA
	Monterey Bay	1987	

Salinity	Bodega Marine Lab	1988	Bodega Ocean Observing Node, Bodega Marine Lab, University of California Davis
	Farallon Islands	1955	Scripps Institution of Oceanography Shore Stations Program
Air Temperature	Fort Ross	1950	National Climate Data Center, NOAA
	Bodega Marine Lab	1988	Bodega Ocean Observing Node, Bodega Marine Lab, University of California Davis
	San Francisco	1959	National Climate Data Center, NOAA
	Pacifica	1984	
	Half Moon Bay	1939	
Precipitation	Fort Ross	1931	National Climate Data Center, NOAA
	San Francisco	1959	
	Pacifica	1984	
	Half Moon Bay	1939	
Biological	Chlorophyll-a Concentration	1997	Mati Kahru, Scripps Photobiology Group, Scripps Institution of Oceanography
	Seabird Reproductive Success	1971, 1972	PRBO Conservation Science

Table 2. Trends based on Spearman rank correlation for physical variables from 1990 to 2010 (n=252), except for current flow which spans 2002 to 2010 (n=108). Shading indicates significance (p<0.05) without adjustment for autocorrelation. Climate indices, the Northern Oscillation Index, California Current flow, and variable type first principal components (PC1s) were subjected to quadratic regression to test for non-linearity in patterns of change (*denotes variables with significant quadratic terms).

		Spearman rho	p-value
Sub-tropical Climate Indices	Southern Oscillation Index*	-0.31	<0.0001
	Multivariate ENSO Index*	-0.31	<0.0001
	Oceanic Nino Index*	-0.20	0.0017
Sub-arctic Climate Indices	North Pacific Index	0.05	0.4571
	North Pacific Gyre Oscillation*	0.52	<0.0001
	Pacific Decadal Oscillation*	-0.25	0.0001
Upwelling	Northern Oscillation Index*	0.27	<0.0001
	Bakun Upwelling Index 36°N	0.11	0.0813
	Bakun Upwelling Index 39°N	0.17	0.0084
	Bakun Upwelling Index PC1*	0.16	0.0132
California Current Flow	California Current	0.14	0.1639
	Point Reyes Cell 0	0.08	0.4329
	Point Reyes Cell 1	0.12	0.2239
	Point Reyes Cell 2	0.19	0.0436
	Point Reyes Cell 3	0.08	0.4395
	Point Reyes Flow PC1	0.12	0.2070
Wind Stress	Bodega Bay	0.13	0.0331
	San Francisco	0.20	0.0014
	Half Moon Bay	0.18	0.0046
	Monterey Bay	0.15	0.0185
	Wind Stress PC1*	0.18	0.0051
Sea Level	South Beach	0.03	0.6420
	Crescent City	-0.27	<0.0001
	San Francisco	0.00	0.9947
	Sea Level PC1	-0.09	0.1578
Sea Surface Temperature	Point Arena	-0.24	0.0002
	Bodega Marine Lab	-0.08	0.1961
	Bodega Bay	-0.17	0.0060
	San Francisco	-0.09	0.1495
	Farallon Islands	-0.20	0.0011
	Half Moon Bay	-0.17	0.0071
	Monterey Bay	0.02	0.7585
	SST PC1*	-0.17	0.0061
Salinity	Bodega Marine Lab	0.08	0.1885
	Farallon Islands	0.01	0.8509
	Salinity PC1*	0.08	0.1936
Air Temperature	Fort Ross	-0.03	0.6805
	Bodega Marine Lab	-0.35	<0.0001
	San Francisco	-0.20	0.0012
	Pacifica	0.17	0.0075
	Half Moon Bay	-0.07	0.2865
	Air Temperature PC1*	-0.15	0.0154

Precipitation	Fort Ross	0.06	0.3673
	San Francisco	0.04	0.4828
	Pacifica	0.01	0.9201
	Half Moon Bay	0.00	0.9986
	Precipitation PC1	0.02	0.7403

Table 3. Results of principal components analysis within variable types, 1990-2010 (Pt. Reyes surface flow, 2002-2010). A. Eigenvalues and variance explained by the first two principal components. B. Site loadings within variable type.

A.

	Component	Eigenvalue	Proportion	Cumulative
Bakun Upwelling	1	1.701	0.850	0.850
	2	0.299	0.150	1.000
Surface Flow, Pt. Reyes	1	3.349	0.837	0.837
	2	0.467	0.117	0.954
Wind Stress	1	3.287	0.822	0.822
	2	0.405	0.101	0.923
Sea level	1	2.545	0.848	0.848
	2	0.309	0.103	0.951
Sea Surface Temperature	1	4.989	0.713	0.713
	2	0.559	0.080	0.793
Salinity	1	1.734	0.867	0.867
	2	0.266	0.133	1.000
Air Temperature	1	3.235	0.647	0.647
	2	0.723	0.153	0.800
Precipitation	1	3.660	0.915	0.915
	2	0.157	0.039	0.954

B.

		Eigenvector Loadings	
	Site	1	2
Bakun Upwelling	36°N	0.707	0.707
	39°N	0.707	-0.707
Surface Flow, Pt. Reyes	Cell 0	0.478	0.626
	Cell 1	0.514	0.334
	Cell 2	0.523	-0.321
	Cell 3	0.484	-0.627
Wind Stress	Bodega Bay	0.513	0.016
	San Francisco	0.465	0.815
	Half Moon Bay	0.514	-0.344
	Monterey Bay	0.507	-0.462
Sea level	South Beach	0.573	-0.642
	Crescent City	0.596	-0.101
	San Francisco	0.563	0.760
Sea Surface Temperature	Point Arena	0.356	-0.628
	Bodega Marine Lab	0.399	-0.176
	Bodega Bay	0.387	0.124
	San Francisco	0.404	0.065
	Farallon Islands	0.407	-0.138
	Half Moon Bay	0.347	0.729
	Monterey Bay	0.338	0.068
Salinity	Farallon Islands	0.707	0.707
	Bodega Marine Lab	0.707	-0.707
Air Temperature	Fort Ross	0.478	-0.005
	Bodega Marine Lab	0.401	-0.620
	San Francisco	0.490	0.018

	Pacifica	0.368	0.779
	Half Moon Bay	0.485	-0.092
Precipitation	Fort Ross	0.491	0.857
	San Francisco	0.499	-0.142
	Pacifica	0.507	-0.297
	Half Moon Bay	0.503	-0.396

Table 4. Interrelationships between environmental indicators. Spearman rank cross-correlations (Spearman rho) for monthly anomalies of climate indicators and first principal components of ocean indicators based on monthly anomalies, 1990-2010 (n=252) or current flow (2002-2010, n=108). Shading indicates rho > |0.5|.

	Multivariate ENSO Index	Southern Oscillation Index	Oceanic Nino Index	North Pacific Index	North Pacific Gyre Oscillation	Pacific Decadal Oscillation	Northern Oscillation Index
Southern Oscillation Index	0.76						
Oceanic Nino Index	0.93	0.74					
North Pacific Index	-0.28	-0.27	-0.30				
North Pacific Gyre Oscillation	-0.40	-0.33	-0.32	-0.04			
Pacific Decadal Oscillation	0.51	0.39	0.46	-0.34	-0.40		
Northern Oscillation Index	-0.51	-0.50	-0.48	0.44	0.25	-0.40	
Upwelling Index PC1	-0.26	-0.12	-0.23	0.33	0.19	-0.34	0.60
California Current Flow	-0.40	-0.38	-0.43	0.09	0.30	-0.43	0.33
Surface Flow, Pt. Reyes PC1	-0.22	-0.15	-0.24	0.10	0.02	-0.10	0.54
Wind Stress PC1	-0.18	-0.11	-0.16	0.25	0.18	-0.24	0.61
Sea Level PC1	0.46	0.31	0.42	-0.38	-0.29	0.50	-0.76
Sea Surface Temperature PC1	0.43	0.30	0.37	-0.33	-0.38	0.59	-0.60
Salinity PC1	-0.20	-0.08	-0.15	0.20	0.31	-0.48	0.38
Air Temperature PC1	0.25	0.24	0.21	-0.32	-0.23	0.51	-0.45
Precipitation PC1	0.01	-0.04	-0.01	-0.12	0.00	0.10	-0.37

	Upwelling Index PC1	California Current Flow	Surface Flow, Pt. Reyes PC1	Wind Stress PC1	Sea Level PC1	Sea Surface Temperature PC1	Salinity PC1	Air Temperature PC1
California Current Flow	0.22							
Surface Flow, Pt. Reyes PC1	0.33	0.10						
Wind Stress PC1	0.66	0.18	0.59					
Sea Level PC1	-0.66	-0.39	-0.43	-0.55				
Sea Surface Temperature PC1	-0.57	-0.39	-0.40	-0.54	0.70			
Salinity PC1	0.37	0.40	0.12	0.38	-0.62	-0.57		
Air Temperature PC1	-0.41	-0.24	-0.06	-0.34	0.44	0.69	-0.39	
Precipitation PC1	-0.41	-0.12	-0.33	-0.47	0.50	0.18	-0.28	0.04

Table 5. Seasonal multivariate ocean-climate indicators (MOCI) derived by principal component analysis (PCA) on detrended physical variables within each season, 1990-2010. A. Eigenvalues and proportion explained for the first and second principal components. B. Eigenvector loadings for first and second principal components by season. Shading indicates values > |0.2|.

A.

Season	Component	Eigenvalue	Proportion	Cumulative
Winter	1	18.943	0.557	0.557
	2	5.000	0.147	0.704
Spring	1	18.163	0.534	0.534
	2	4.628	0.136	0.670
Summer	1	13.025	0.383	0.383
	2	4.673	0.138	0.521
Fall	1	13.729	0.404	0.404
	2	4.084	0.120	0.524

B.

		Winter		Spring		Summer		Fall	
		1	2	1	2	1	2	1	2
Sub-tropical Climate Indices	Southern Oscillation Index	0.149	0.113	0.063	0.248	0.111	-0.200	0.148	0.305
	Multivariate ENSO Index	0.164	0.087	0.151	0.151	0.193	-0.132	0.147	0.330
	Oceanic Nino Index	0.161	0.120	0.125	0.191	0.176	-0.195	0.135	0.364
Sub-arctic Climate Indices	North Pacific Index	-0.145	0.014	-0.078	-0.206	-0.182	0.199	-0.090	-0.091
	North Pacific Gyre Oscillation	-0.073	-0.162	-0.147	-0.097	-0.071	-0.129	-0.102	0.036
	Pacific Decadal Oscillation	0.157	0.206	0.182	0.028	0.196	0.031	0.219	0.012
Upwelling	Northern Oscillation Index	-0.218	0.046	-0.191	-0.122	-0.164	0.185	-0.207	-0.262
	Bakun Upwelling Index 36°N	-0.174	0.017	-0.192	-0.002	-0.136	-0.057	-0.122	-0.068
	Bakun Upwelling Index 39°N	-0.193	0.111	-0.211	-0.008	-0.189	0.081	-0.110	0.074
Wind Stress	Bodega Bay	-0.193	0.119	-0.180	0.083	-0.076	0.265	-0.196	0.195
	San Francisco	-0.193	0.147	-0.191	0.106	-0.027	0.152	-0.199	0.181
	Half Moon Bay	-0.190	0.139	-0.141	0.011	0.052	0.218	-0.187	0.151
	Monterey Bay	-0.177	0.137	-0.191	0.071	0.007	0.225	-0.204	0.081
Sea Level	South Beach	0.200	-0.142	0.199	0.001	0.251	-0.008	0.169	0.224
	Crescent City	0.219	-0.086	0.222	0.017	0.235	0.039	0.212	0.172
	San Francisco	0.213	-0.089	0.202	-0.102	0.179	0.203	0.225	0.224
Sea Surface Temperature	Point Arena	0.192	0.057	0.184	0.048	0.236	-0.070	0.198	-0.042
	Bodega Marine Lab	0.204	0.129	0.209	0.037	0.210	0.070	0.220	-0.034
	Bodega Bay	0.196	0.165	0.222	-0.034	0.173	0.213	0.194	-0.159
	San Francisco	0.188	0.157	0.211	0.087	0.242	0.141	0.219	-0.106
	Farallon Islands	0.215	0.092	0.204	0.024	0.240	0.092	0.218	-0.019
	Half Moon Bay	0.148	0.166	0.168	0.065	0.184	0.233	0.171	-0.211
	Monterey Bay	0.171	0.187	0.184	-0.055	0.205	0.098	0.144	0.004
Salinity	Bodega Marine Lab	-0.170	0.125	-0.169	0.138	-0.158	-0.038	-0.129	0.164
	Farallon Islands	-0.138	0.059	-0.183	0.179	-0.124	-0.261	-0.103	0.200
Air Temperature	Fort Ross	0.169	0.169	0.162	0.191	0.199	0.059	0.157	-0.121
	Bodega Marine Lab	0.151	0.178	0.172	0.151	0.094	0.115	0.197	-0.180
	San Francisco	0.150	0.169	0.184	0.169	0.226	0.057	0.167	-0.205
	Pacifica	0.086	0.316	0.024	0.371	0.213	-0.006	0.099	-0.209
	Half Moon Bay	0.179	0.149	0.189	0.138	0.224	-0.029	0.190	-0.076
Precipitation	Fort Ross	0.138	-0.287	0.166	-0.244	0.131	-0.207	0.118	0.144
	San Francisco	0.144	-0.315	0.087	-0.359	0.133	-0.271	0.130	0.138
	Pacifica	0.129	-0.338	0.122	-0.358	0.092	-0.330	0.155	0.115
	Half Moon Bay	0.129	-0.323	0.108	-0.381	0.055	-0.327	0.180	0.066

Table 6. Cross-correlation of seasonal MOCI produced by principal component analysis (PCA), local variables only combined with PCA, and climate indices only combined with PCA. In each cell, Spearman rho is the top value and the p-value is below. Shading indicates significance (p<0.05). Winter, spring, and summer n = 21; fall n = 20.

	$Fall_{x-1}$		Winter		Spring		Summer	
	MOCI	Local Variables	MOCI	Local Variables	MOCI	Local Variables	MOCI	Local Variables
Local Variables	0.97 <0.0001		0.98 <0.0001		0.99 <0.0001		0.97 <0.0001	
Climate Indices	0.71 0.0001	0.65 0.0018	0.78 <0.0001	0.73 0.0002	0.73 0.0002	0.67 0.0009	0.53 0.0130	0.43 0.0542

Table 7. Spearman rank correlations of seabird reproductive success residuals and $PC1_{seabirds}$ and seasonal MOCI. In each cell are Spearman rho and p-value. N = 18 for all relationships. Shading indicates relationships where $p < 0.05$.

	MOCI1-Winter	MOCI2-Winter	MOCI1-Spring	MOCI2-Spring	MOCI1-Summer	MOCI2-Summer	MOCI1-Fall	MOCI2-Fall
Common Murre	-0.59	-0.10	-0.73	0.04	0.01	-0.57	-0.31	0.15
	0.01	0.70	<0.01	0.87	0.98	0.01	0.21	0.55
Pigeon Guillemot	-0.35	-0.03	-0.62	0.25	-0.13	-0.59	0.16	0.27
	0.16	0.92	0.01	0.32	0.60	0.01	0.53	0.28
Cassin's Auklet	-0.19	-0.09	-0.48	-0.06	-0.50	-0.38	-0.17	0.29
	0.45	0.73	0.04	0.82	0.03	0.12	0.51	0.24
Brandt's Cormorant	-0.33	-0.13	-0.61	-0.22	-0.39	-0.66	-0.21	0.16
	0.18	0.60	0.01	0.38	0.11	<0.01	0.40	0.53
$PC1_{seabirds}$	-0.48	-0.13	-0.79	0.01	-0.44	-0.68	-0.15	0.28
	0.04	0.62	<0.01	0.96	0.07	<0.01	0.55	0.26

Figure 1. Indicators of El Niño/La Niña, transport from the tropics. A. Southern Oscillation Index (SOI, sign reversed), B. Multivariate ENSO Index (MEI), and C. Oceanic Niño Index (ONI), 1990-2010. Blue line indicates LOESS smoothing function with sampling proportion of 0.2. Dashed lines show +/- 1 long-term standard deviation based on varying time series (SOI: 1900-2010, MEI and ONI: 1950-2010).

A.

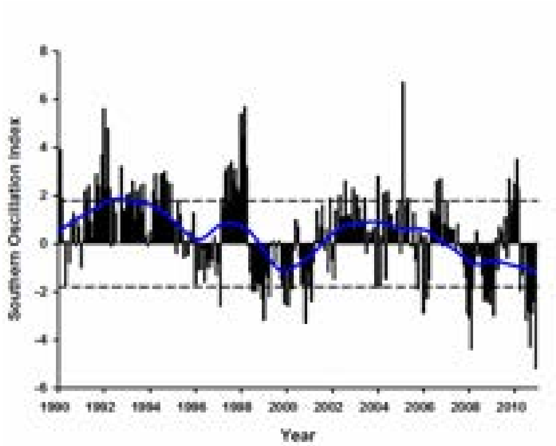

B.

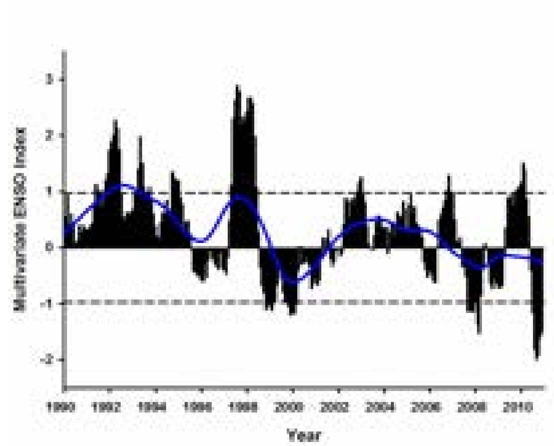

C.

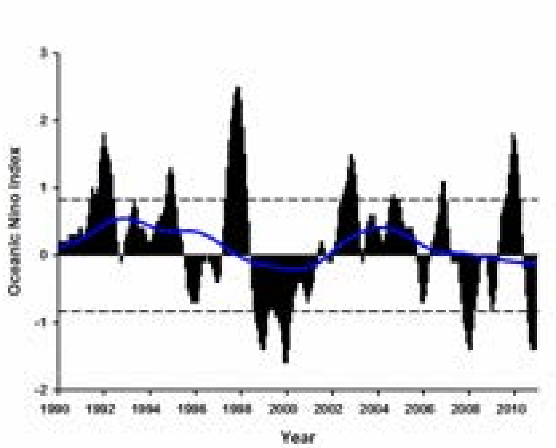

Figure 2. Indicators of transport from the sub-arctic North Pacific. A. North Pacific Index (NPI) monthly anomalies, B. Pacific Decadal Oscillation (PDO), and C. North Pacific Gyre Oscillation Index (NPGO), 1990-2010. Blue line indicates LOESS smoothing function with sampling proportion of 0.2. Dashed lines show +/- 1 long-term standard deviation based on varying time series (NPI and PDO: 1900-2010 and NPGO: 1950-2010).

A.

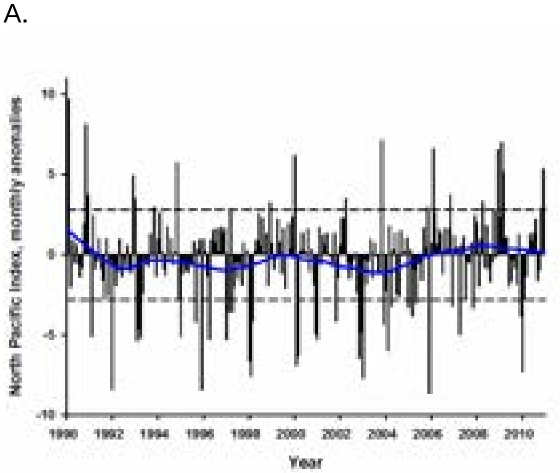

B.

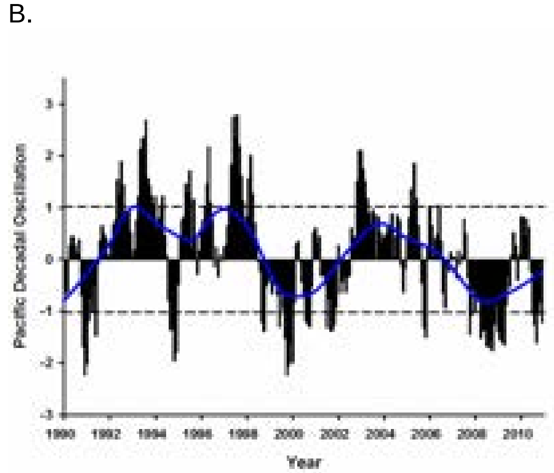

C.

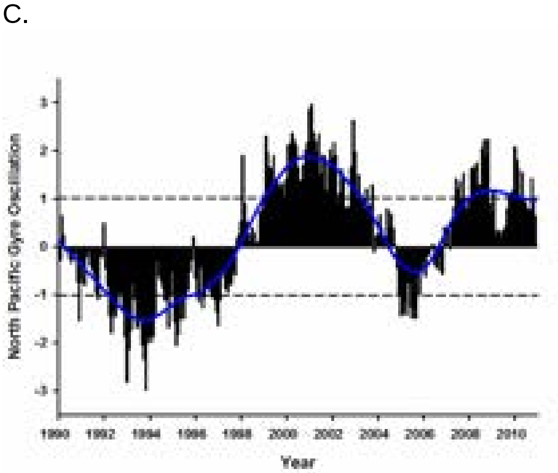

Figure 3. A. Indicators of regional upwelling. Northern Oscillation Index (NOI) and B. the first principal component (PC1) of Bakun Upwelling Index at 36°N and 39°N, 1990-2010. Blue line indicates LOESS smoothing function with sampling proportion of 0.2. Dashed lines show +/- 1 long-term standard deviation for NOI (1970-2010) and 1990-2010 standard deviation for Upwelling PC1.

A.

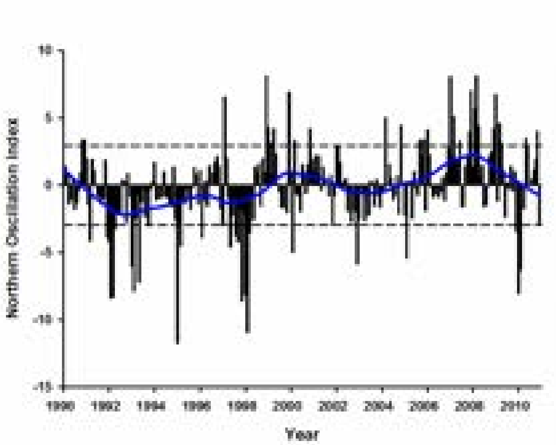

B.

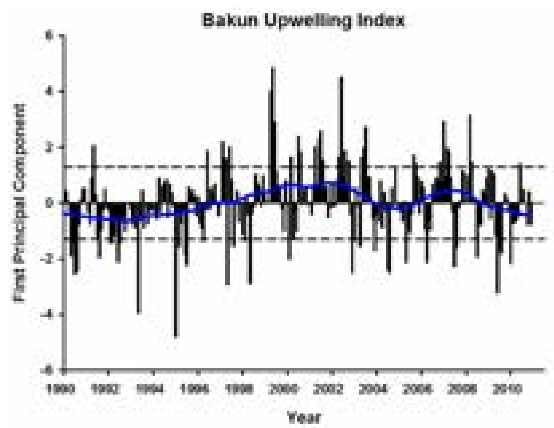

Figure 4. Indicators of large-scale and local current flow. A. California Current flow measured by Argo and B. surface flow at Pt. Reyes, first principal component of all cells, 2002-2010. Blue line indicates LOESS smoothing function with sampling proportion of 0.2. Dashed lines show +/- 1 standard deviation.

A.

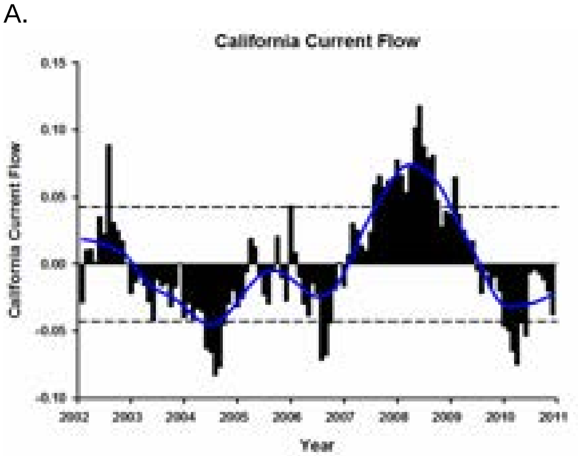

B.

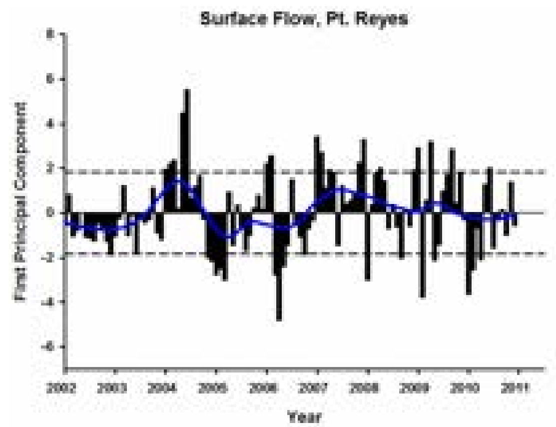

Figure 5. Indicators of regional coupled wind and hydrography (1990-2010): A. wind stress, B. sea surface temperature, C. sea level, and D. salinity. Blue line indicates LOESS smoothing function with sampling proportion of 0.2. Dashed lines show +/- 1 standard deviation.

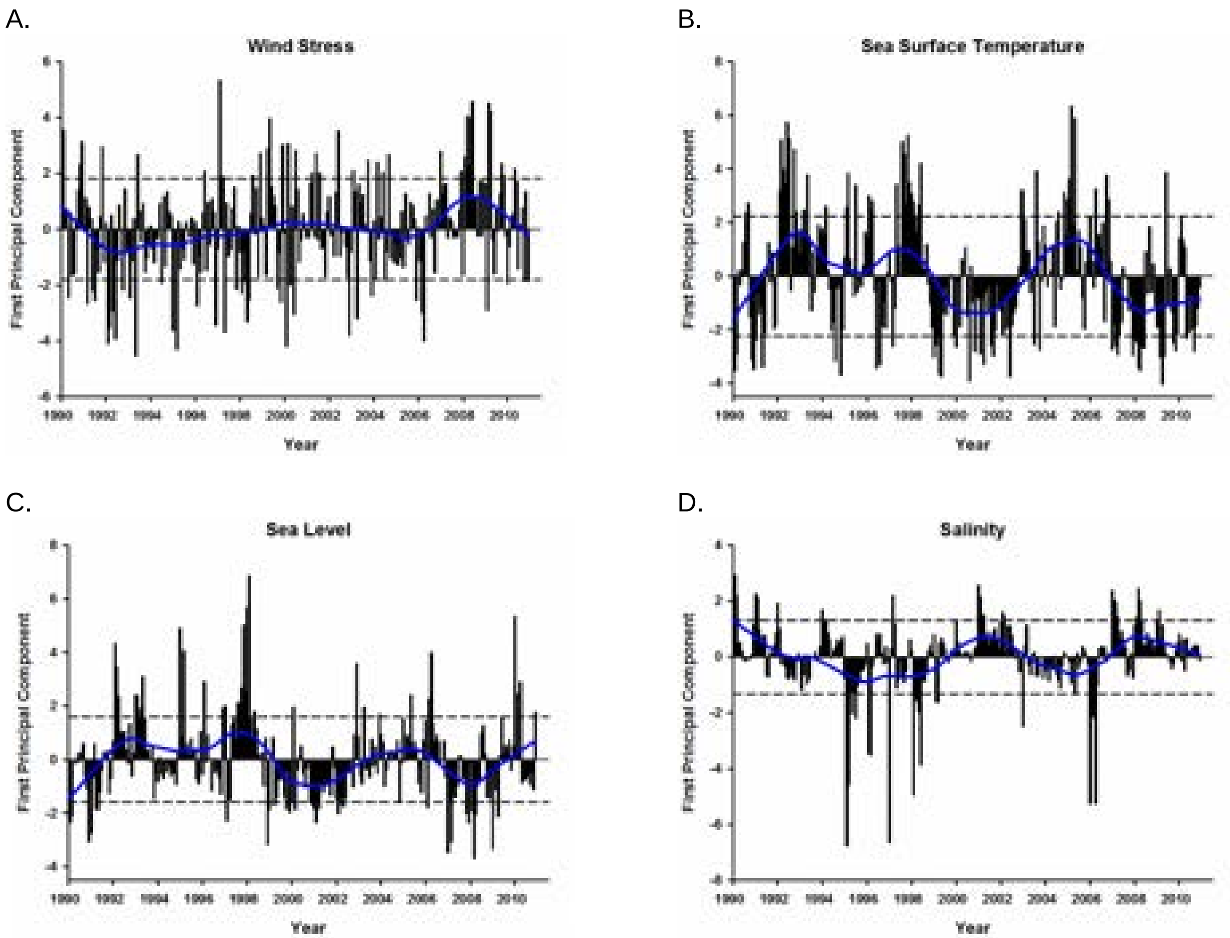

Figure 6. Indicators of regional atmospheric conditions. First principal components of A. air temperature and B. precipitation, 1990-2010. Blue line indicates LOESS smoothing function with sampling proportion of 0.2. Dashed lines show +/- 1 standard deviation.

A.

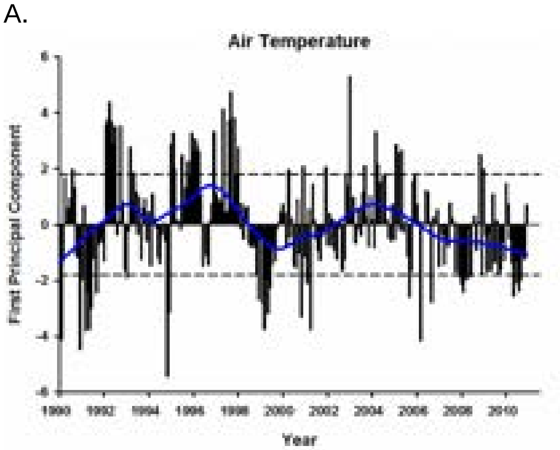

B.

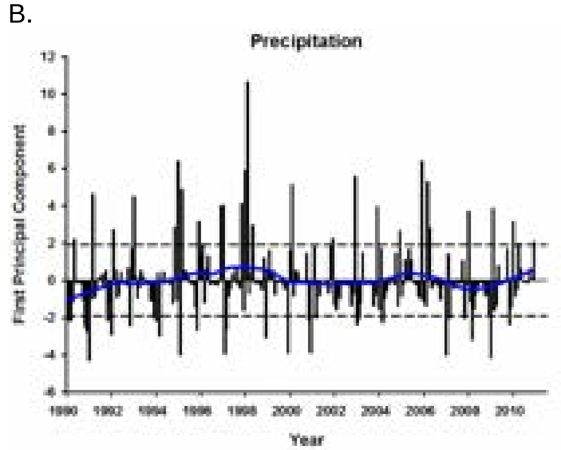

Figure 7. The first principal component variable loadings plotted against the second principal component variable loadings (PC space), 1990-2010 for seasonal MOCI. MOCI were calculated from residuals of seasonal averages. A. winter, B. spring, C. summer, and D. fall. Labels for circular symbols indicate climate variables. SOI: Southern Oscillation Index; MEI: Multivariate ENSO Index; NOI: Northern Oscillation Index; NPGO: North Pacific Gyre Oscillation; NPI: North Pacific Index; ONI: Oceanic Nino Index; PDO: Pacific Decadal Oscillation. ☆✚: sea level; ■: sea surface temperature (SST); **x**: salinity; ▼: Bakun Upwelling Index; : wind stress; ▲: air temperature; ♦: precipitation.

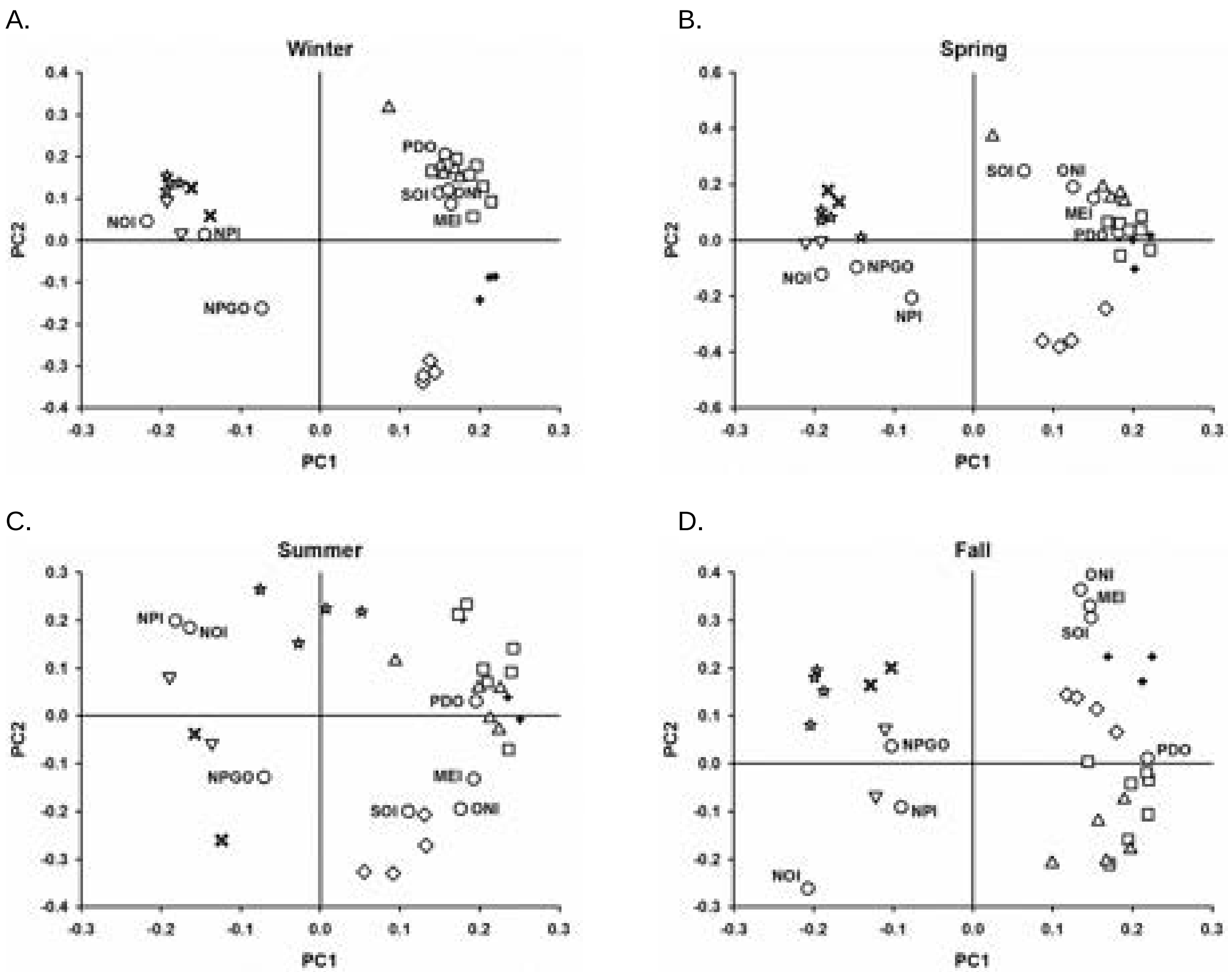

Figure 8. Seasonal MOCI against time for A. winter, B. spring, C. summer and D. fall, 1990-2010. MOCI were calculated from residuals of seasonal averages. Blue line shows LOESS smoothing function with sampling proportion = 0.3. Dashed lines show +/- 1 standard deviation.

A.

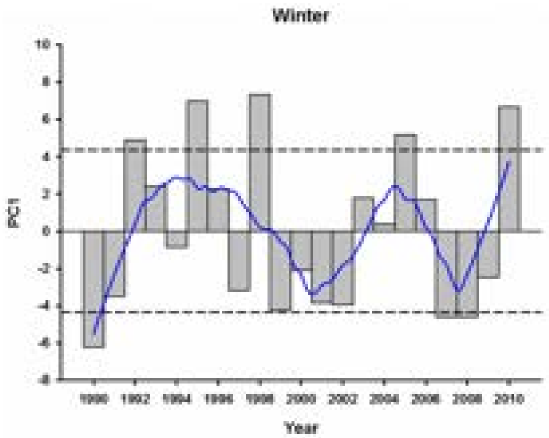

B.

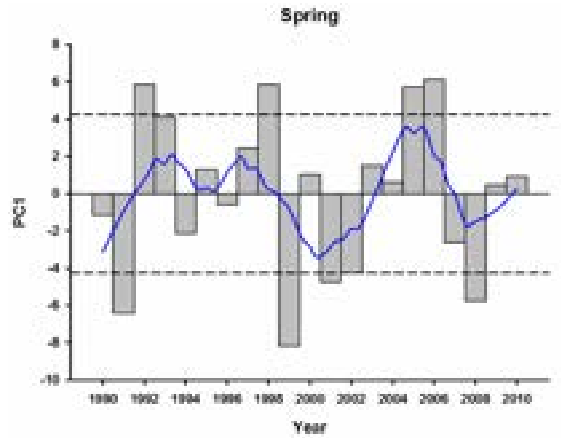

C.

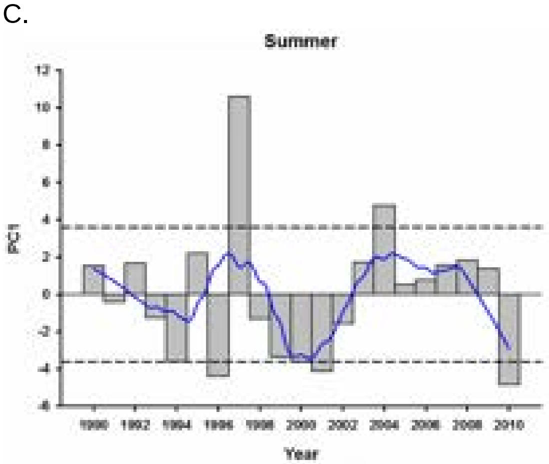

D.

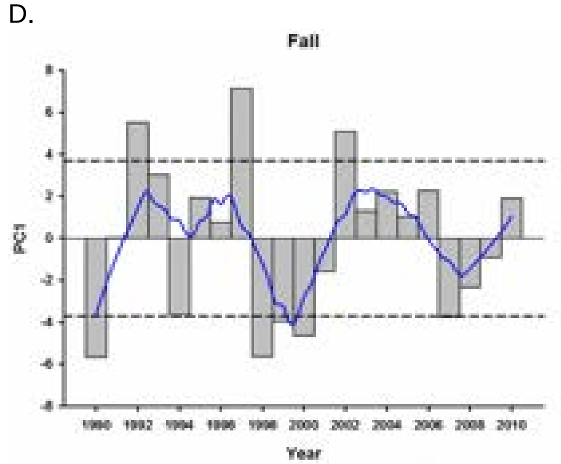

Figure 9. Seasonal MOCI time series, 1990-2010. Smoothed line is based on LOESS with sampling proportion of 0.3. Dashed lines are 1 s.d. for the time series. 1 standard deviation was also calculated for each season. Red points indicate values greater than 1 seasonal s.d. and blue points indicate values less than 1 seasonal s.d.

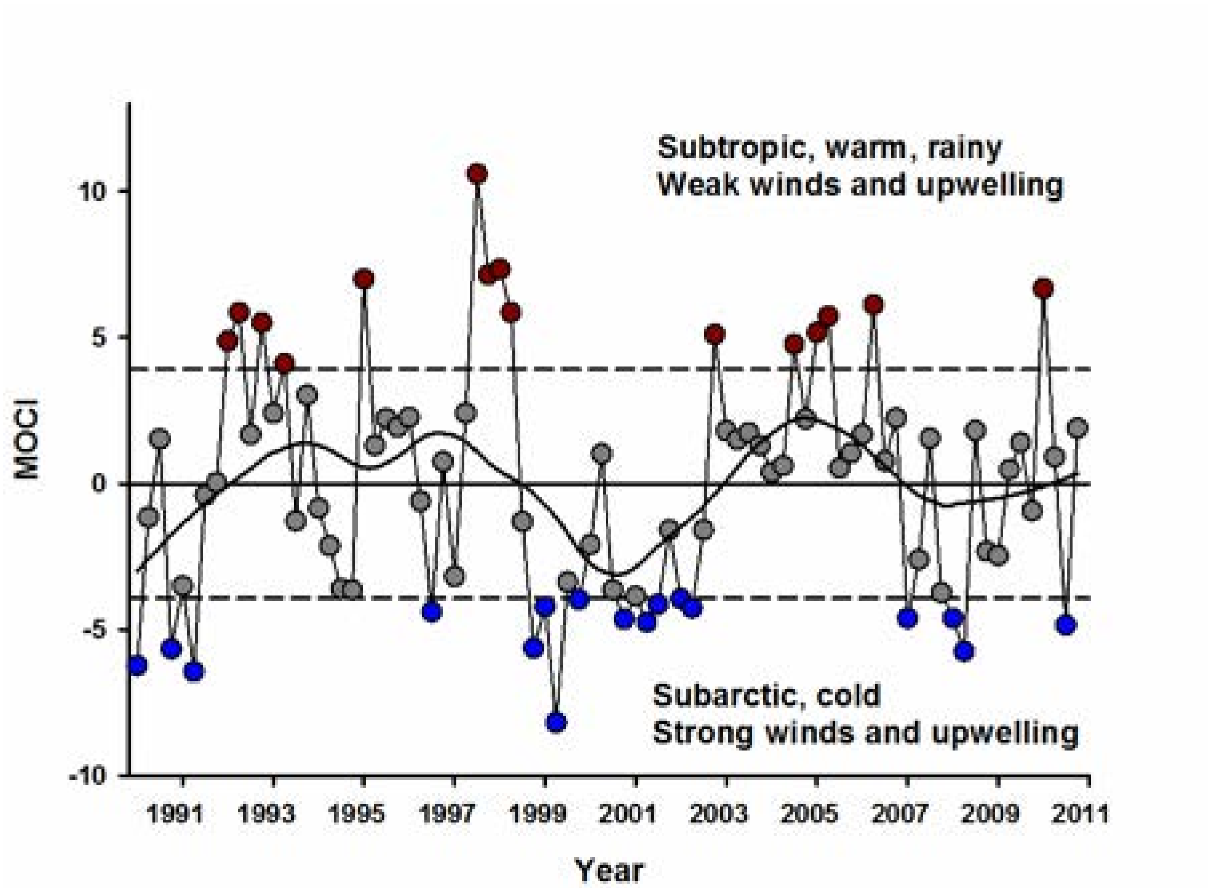

Figure 10. A. Log chlorophyll-a abundance anomalies (1997-2011). Blue line indicates LOESS smoothing function with sampling proportion of 0.3. Dashed lines show +/- 1 standard deviation. Seabird reproductive success with linear regression for B. pigeon guillemot (1971-2007), C. Cassin's auklet (1971-2007), D. common murre (1972-2007), and E. Brandt's cormorant (1971-2007). F. Seabird first principal component, 1972-2007.

A.

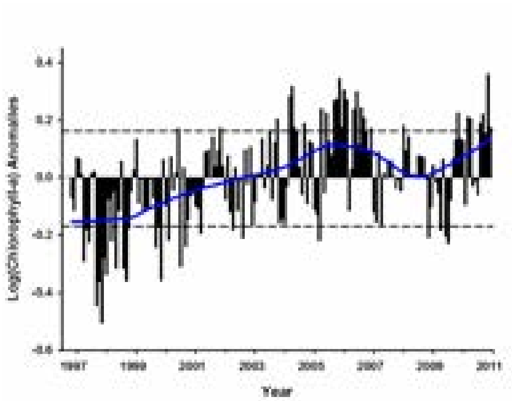

B.

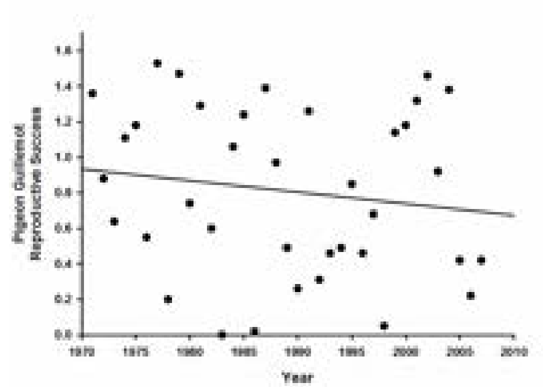

C.

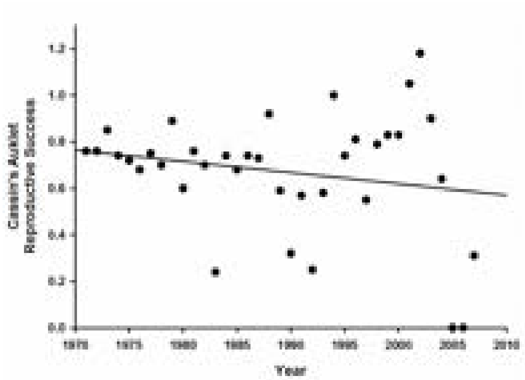

D.

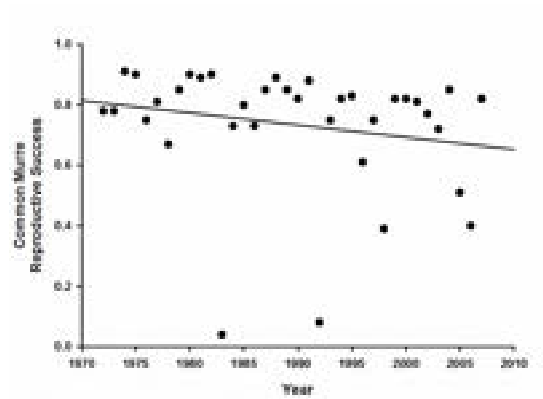

E.

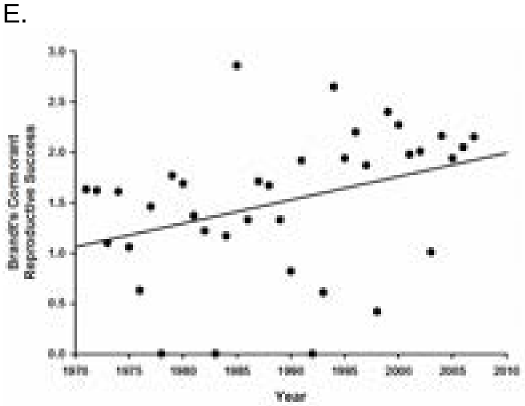

F.

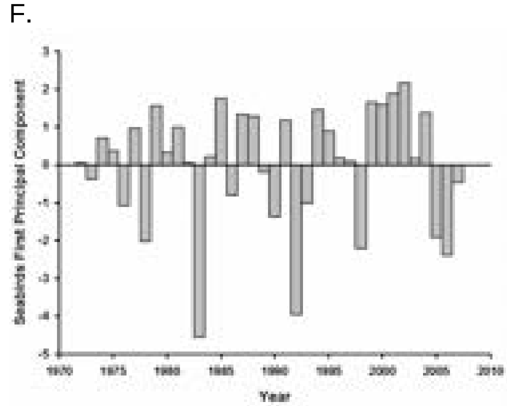

Figure 11. Significant relationships for spring MOCI (PC1) and residuals of reproductive success for A. Cassin's auklet, B. common murre, C. pigeon guillemot, and D. Brandt's Cormorant. E. Relationship of MOCI1-spring and a $PC1_{seabirds}$. Regression lines are linear with the exception of common murre, which is an exponential curve.

A.

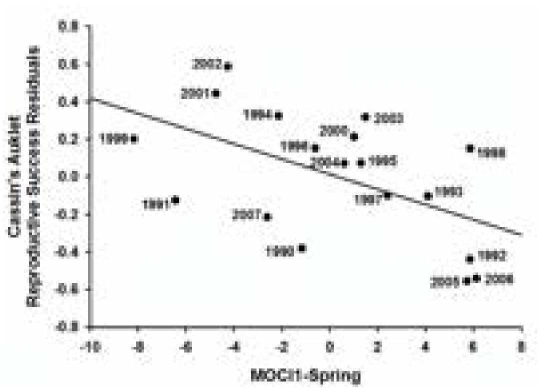

B.

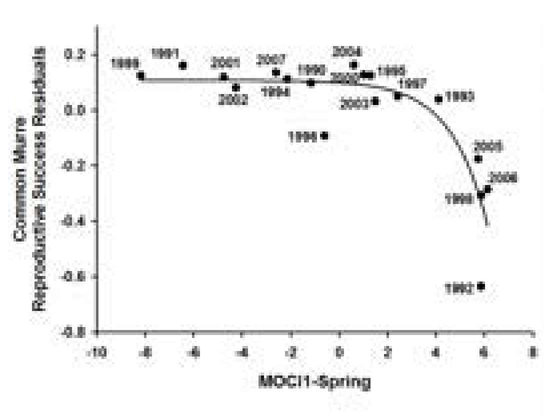

C.

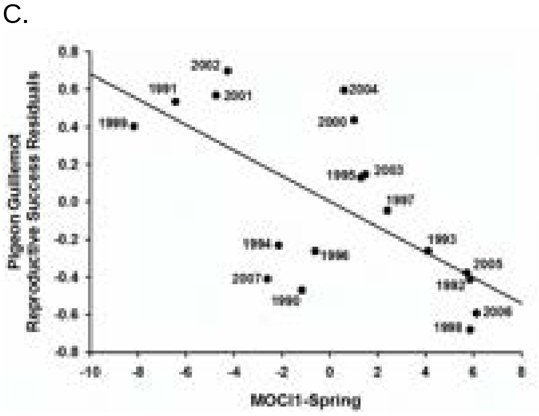

D.

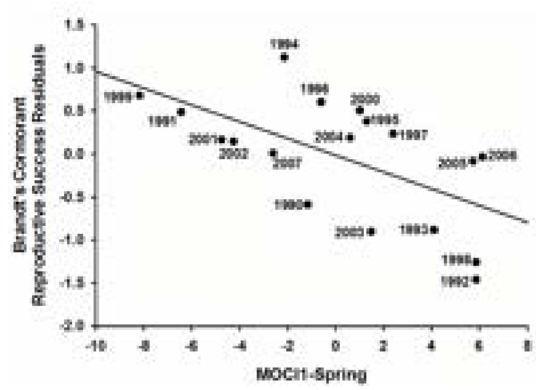

E.